

Crustal thermal processes & Low-T thermochronology in Fennoscandia

Ilmo Kukkonen

*Lecture on the
Short course on low temperature thermochronology*

*University of Helsinki
Oct 23 – 27, 2017*

Crustal thermal processes – Quick overview

Heat flow

Temperatures in crust

Sedimentation and erosion

Intrusions

Extension

Crustal thickening

Low-T thermochronology in Fennoscandia

Geological evolution in central Fennoscandia after the Svecofennian orogeny

Phanerozoic geological history of Fennoscandia

Sedimentary rocks on the peneplain in Fennoscandia

AFT, U-Th/He and Ar-Ar data and models by Murrell

AFT compilation in Fennoscandia by Hendriks et al.

Outokumpu deep drill hole data

Eridanos river system and late erosion

Heat flow from inside the Earth

- Heat flow is determined with Fourier's first law of heat conduction

$$Q = -\lambda \frac{\partial T}{\partial z}$$

- In words the above equation tells that

Heat flow = Thermal conductivity × Temperature gradient

- The common unit applied for heat flow is mW m^{-2}

Conductive temperatures in the crust are calculated by solving Fourier's second law of heat conduction with appropriate boundary conditions

$$\frac{\partial T}{\partial t} = \frac{A}{\rho c} + \frac{\lambda}{\rho c} \frac{\partial^2 T}{\partial z^2}$$

F-2 in 1D

T is *temperature*

t is *time*

A is *heat generation rate* (W m^{-3})

λ is *thermal conductivity which* expresses the ability of matter to conduct heat energy (unit $\text{Wm}^{-1}\text{K}^{-1}$),

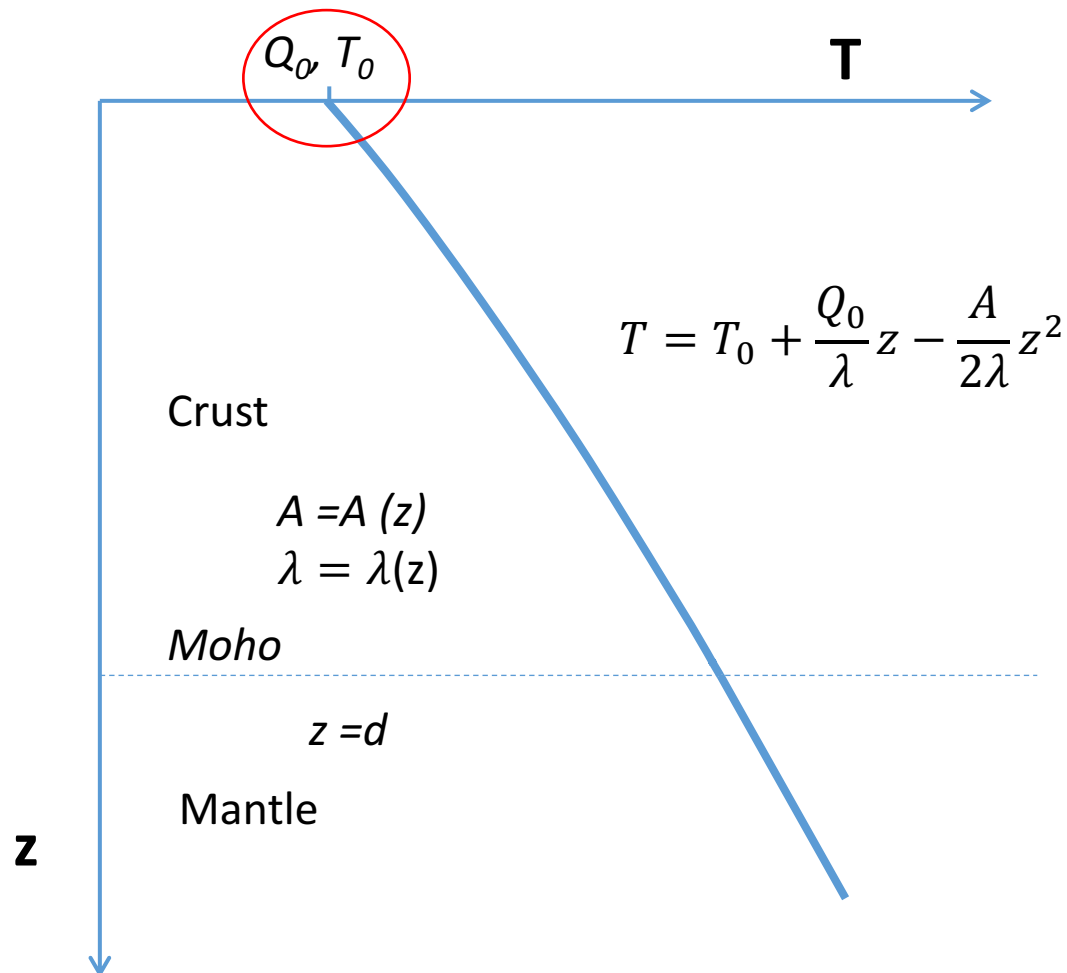
c is *specific heat capacity* (unit $\text{J kg}^{-1}\text{K}^{-1}$) which expresses the ability of matter to store heat

s is *diffusivity* (unit m^2s^{-1}) expresses the ability of matter to react for temperature changes

$$\frac{\lambda}{\rho c} = s$$

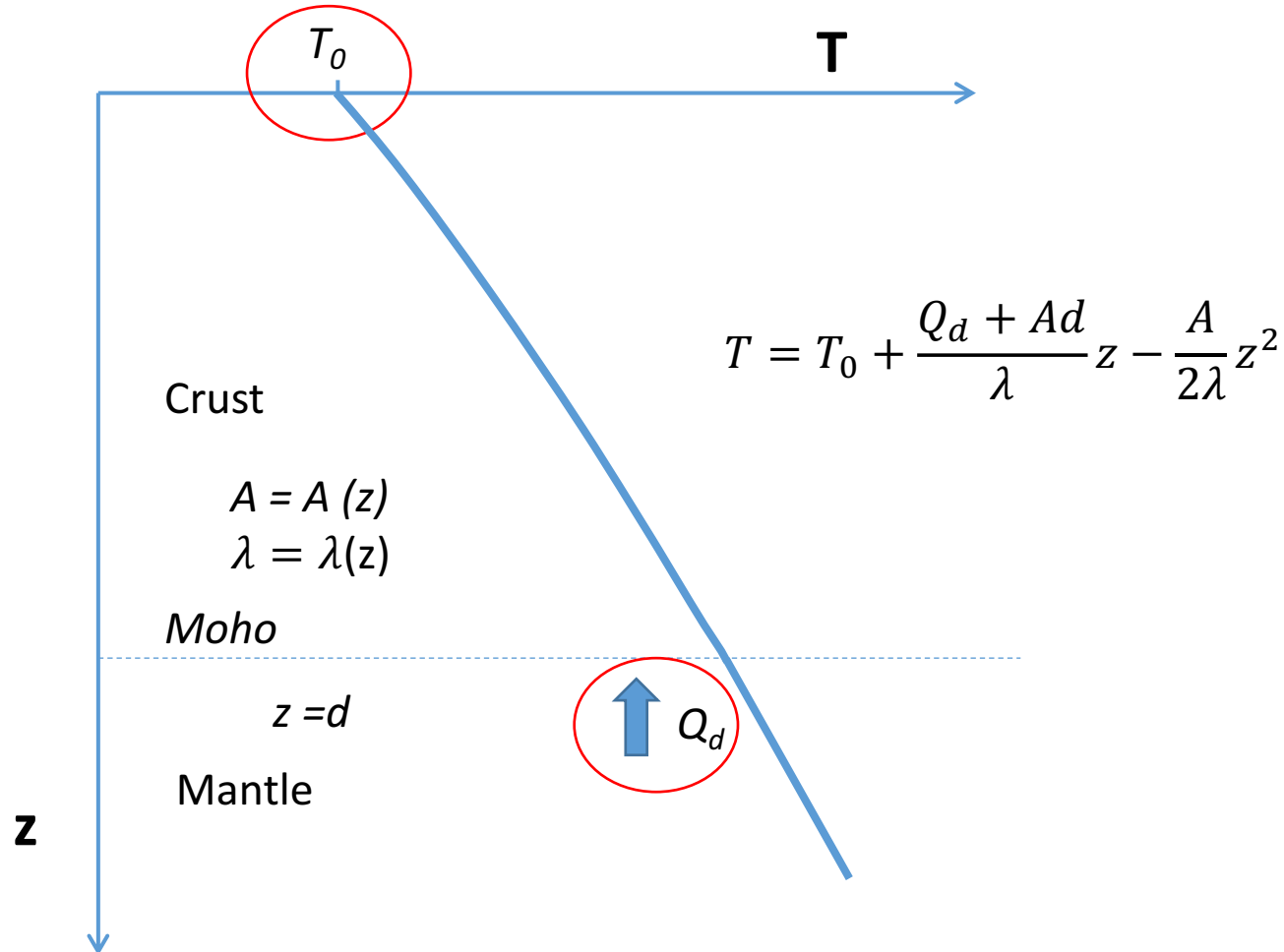
Calculation of crustal temperatures (geotherms)

Alternative 1: Starting from surface heat flow Q_0



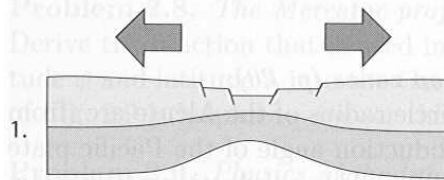
Calculation of crustal temperatures (geotherms) (cont.)

Alternative 2: Starting from mantle heat flow

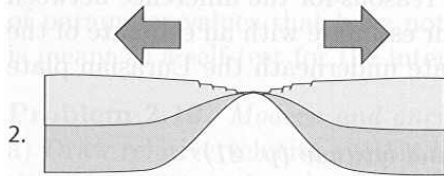


Tectonic phases of the Wilson cycle

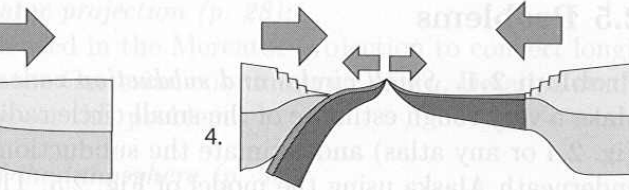
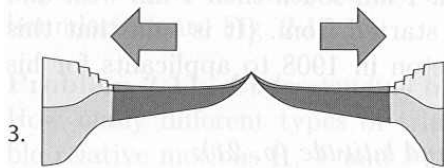
Extension



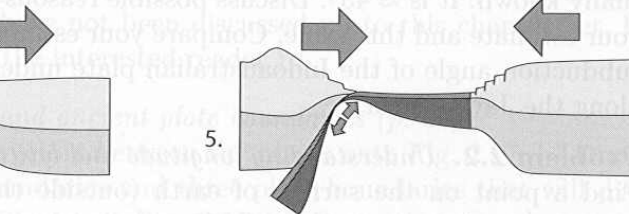
Opening of sea basin



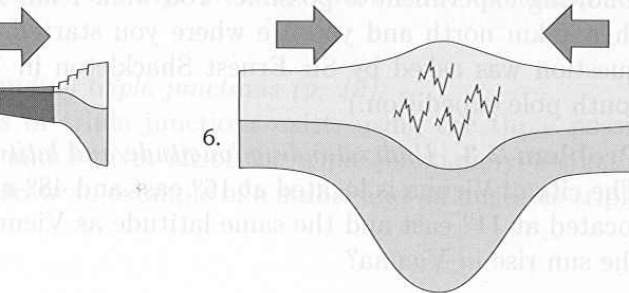
Production of oceanic crust in the mid-oceanic ridge



Subduction of an oceanic plate



Subduction of a ridge



Closure of basin
Collision

Figure 2.21. The Wilson cycle. The arrows indicate the relative plate motions

Stüwe 2002

Duration of conductive thermal disturbances in the lithosphere

$$t = \frac{L^2}{s} \quad (10.1)$$

where

t is the thermal time constant of the lithosphere after which time the disturbances have vanished,

L is lithosphere thickness and

s is diffusivity

Examples

Thick lithosphere :

L = 150 km, $a = 1 \cdot 10^{-6} \text{ m}^2\text{s}^{-1}$, $t = 710 \cdot 10^6 \text{ a}$

Thin lithosphere

L = 50 km, $a = 1 \cdot 10^{-6} \text{ m}^2\text{s}^{-1}$, $t = 80 \cdot 10^6 \text{ a}$

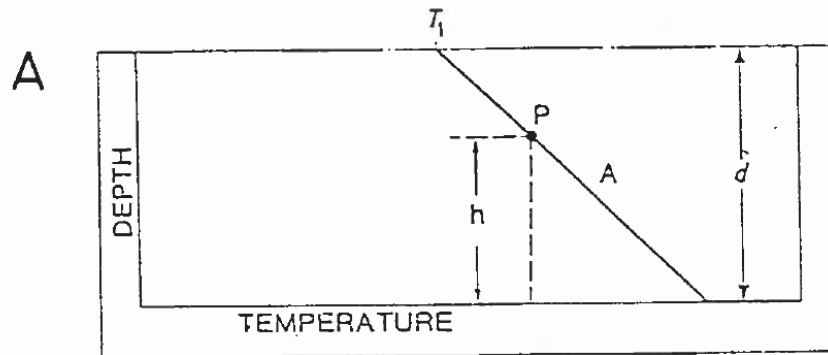
Heat sources in different tectonic processes of the crust

<u>Heat source/mechanism of heat transfer</u>	<u>Importance</u>	<u>Characteristic parameter</u>
Conduction	Big	Characteristic time $\tau = L^2 / s$
Advection		
Fluid flow	small	Peclet number
Magma		$Pe = uL / s$ ($Pe > 1$)
-Intrusions	Big (locally)	
- underplating	Big (locally)	
Erosion, exhumation	Big	
Heat production		
Radioactive	Big	
Chemical		
-latent heat	Big (locally)	$S \times t$
-reactions	Short-lived, local	(S is heat production)

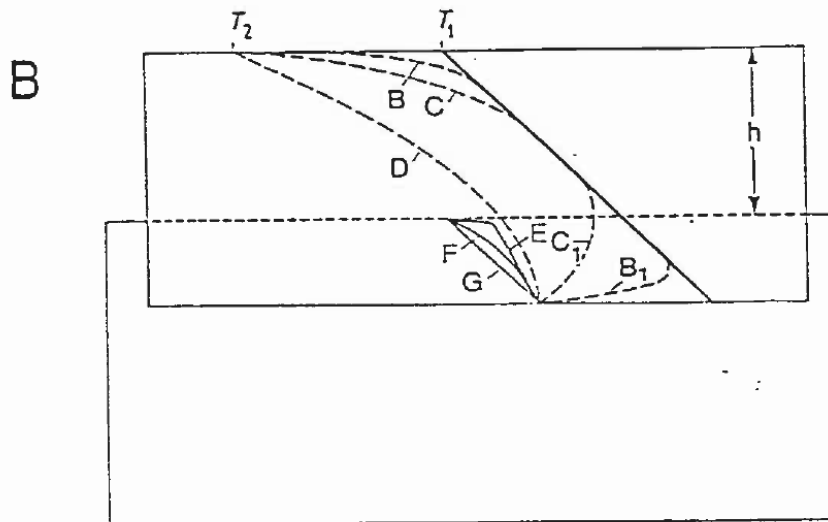
Modified from Stüwe 2002

Effect of erosion, sedimentation and uplift

Effect of uplift and erosion on geotherms



Steady-state temperature profile



Sudden Uplift of block
New T-z curves B, C, D and B₁, C₁

Sudden erosion back to original level
New T-z curves F, G

- The thermal effect of sedimentation and erosion are **analogous to convective heat transfer problems**
- Moving bedrock transports heat with itself
- Heat conduction equation in 1D:

$$s \frac{\partial^2 T}{\partial z^2} = \frac{\partial T}{\partial t} + u \frac{\partial T}{\partial z} \quad (10.2)$$

where

s is diffusivity and

u is the velocity of the medium relative to the boundary surface

(if z is positive downward, **positive velocity is for sedimentation** and **negative for erosion**)

$$T = T_0 + g_b z \quad \text{when } t = 0 \quad (10.3)$$

and when $t > 0$, the surface temperature is

The solution from Carslaw and Jaeger (1959) and repeated by Powell et al. (1988) is:

$$\begin{aligned} T(z, t) &= T_0 + g_b(z - vt) \\ &+ \frac{1}{2} \left[g_b + \frac{g_b u}{v} \right] \times \left[(z + vt) e^{\left(\frac{vz}{s}\right)} \operatorname{erfc} \left(\frac{z + vt}{2\sqrt{st}} \right) - (z - vt) \operatorname{erfc} \left(\frac{z - vt}{2\sqrt{st}} \right) \right] \end{aligned} \tag{10.4}$$

where

u is the (constant) rate of movement of the boundary with respect to a fixed reference (uplift) and

v is the (constant) velocity of the moving medium with respect to a point fixed on the moving boundary (sedimentation, erosion)

g_b is the undisturbed gradient

g_L is the decrease of soil temperature with elevation (lapse rate)

The corresponding effect on temperature gradient is obtained from:

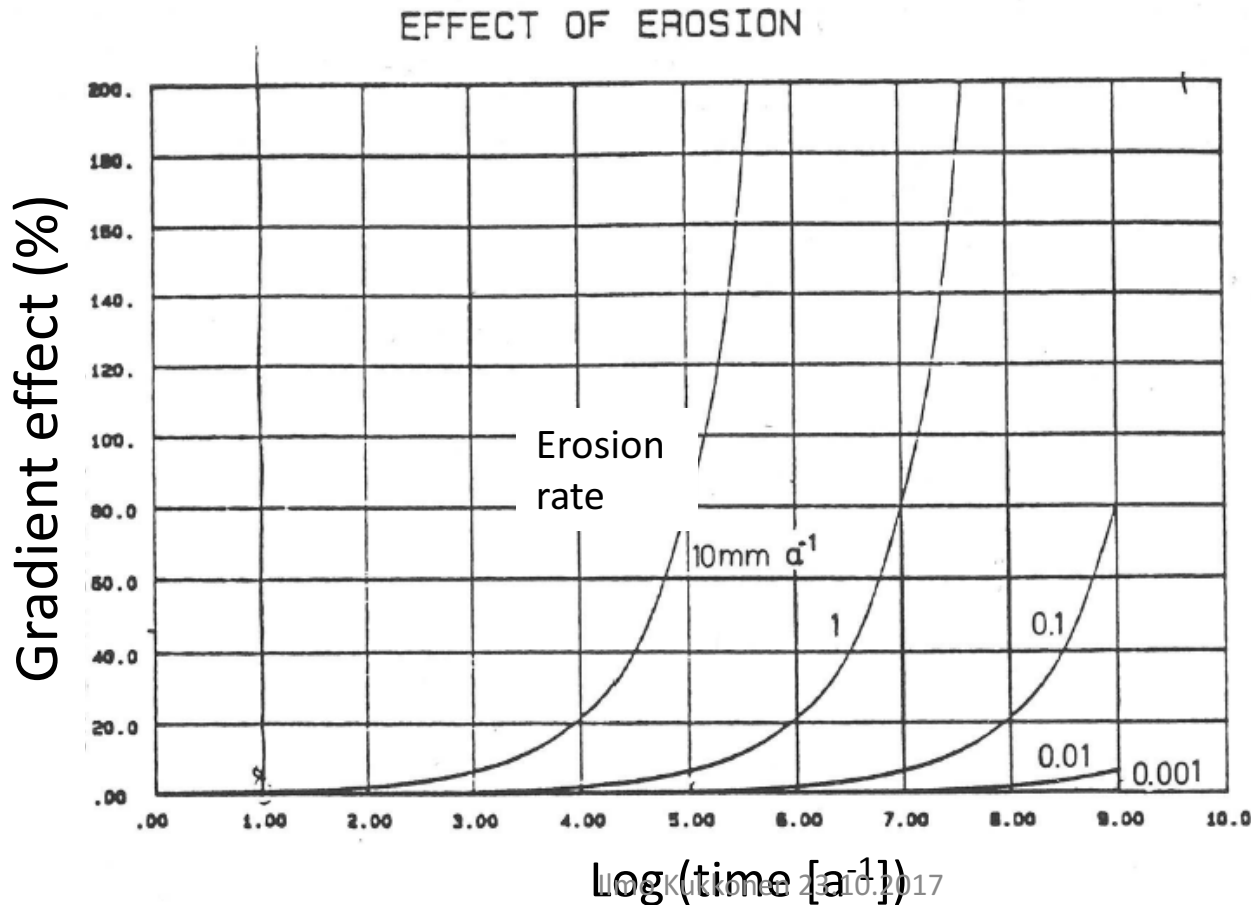
$$\begin{aligned}
 g(z, t) &= \frac{\partial T(z, t)}{\partial z} \\
 &= g_b \frac{1}{2} \left(g_b + \frac{g_L u}{v} \right) \left[-\operatorname{erfc} \left(\frac{z - vt}{2\sqrt{st}} \right) - \frac{z + vt}{\sqrt{\pi st}} e^{\left(\frac{vz}{s}\right)} e^{-\left(\frac{z+vt}{2\sqrt{st}}\right)^2} \right. \\
 &\quad \left. + \frac{z - vt}{\sqrt{\pi st}} e^{-\left(\frac{z-vt}{2\sqrt{st}}\right)^2} + \left(1 + \frac{vz}{s} + \frac{v^2 t}{s} \right) e^{\left(\frac{vz}{s}\right)} \operatorname{erfc} \left(\frac{z + vt}{2\sqrt{st}} \right) \right]
 \end{aligned}$$

(10.5)

Some results for erosion and sedimentation are shown in the next two slides

Effect of erosion on gradient at the earth's surface

- E.g., erosion rate of the Svecofennian mountains (roots presently in southern Finland) was about 0.15 - 0.37 mm/a during 1.84-1.82 Ga
- The erosion rate of mountains decays appr. exponentially with time
- In a system eroding rapidly the surface heat flow is markedly disturbed after times of about 10 - 100 Ma of steady erosion

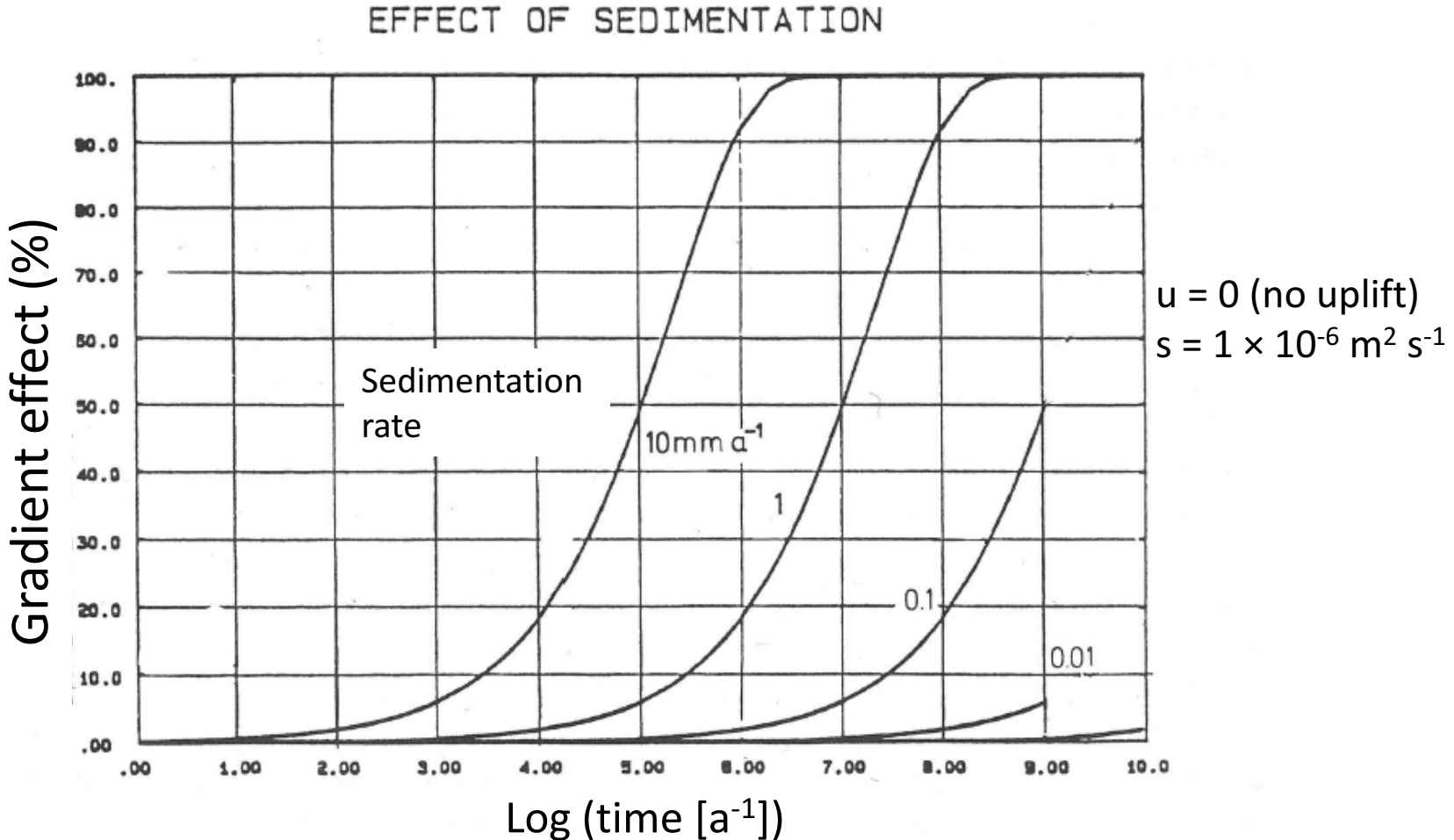


$$u = 0 \text{ (no uplift)}$$
$$s = 1 \times 10^{-6} \text{ m}^2 \text{ s}^{-1}$$

Powell et al. 1988

Effect of sedimentation on gradient at earth's surface

- Typical rates of sedimentation are 1 - 0.1 mm a⁻¹
- The surface heat flow is markedly (>20%) affected only after 1- 100 Ma



Erosion and uplift in a steady-state. The following special cases can be solved in a steady-state condition

1. The upper boundary temperature of the medium (surface temperature) is constant $T_{z=0} = 0$ and the lower boundary temperature is effectively at infinite depth $T_{z \rightarrow \infty} = T_{\infty}$. Then the solution is

$$T = T_{\infty} \left(1 - e^{-\frac{uz}{s}} \right) \quad z \rightarrow \infty \quad (10.6)$$

2. Upper boundary temperature is constant $T_{z=0} = 0$ and lower boundary is at depth $z = L$ (eg., Moho or lithosphere/asthenosphere boundary) is $T = T_L$. Then the solution is

$$T = T_L \left(\frac{1 - e^{-uz/s}}{1 - e^{-uL/s}} \right) \quad (10.7)$$

In the figure (next page) the results of these special cases are shown.

Effect of erosion in steady-state conditions

$$T_{z=0} = 0$$

$$T_{z \rightarrow \infty} = T_{\infty} = 1000^{\circ}\text{C}$$

$$s = 1 \times 10^{-6} \text{ m}^2 \text{ s}^{-1}$$

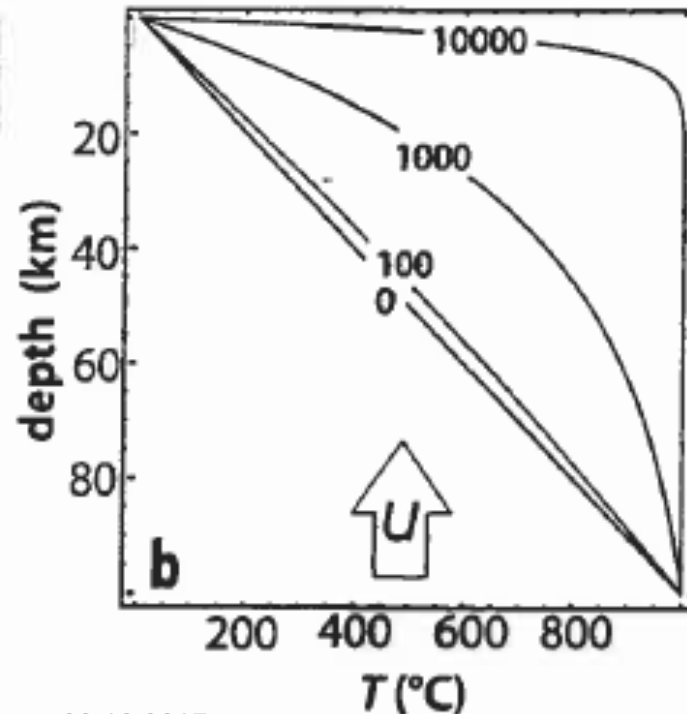
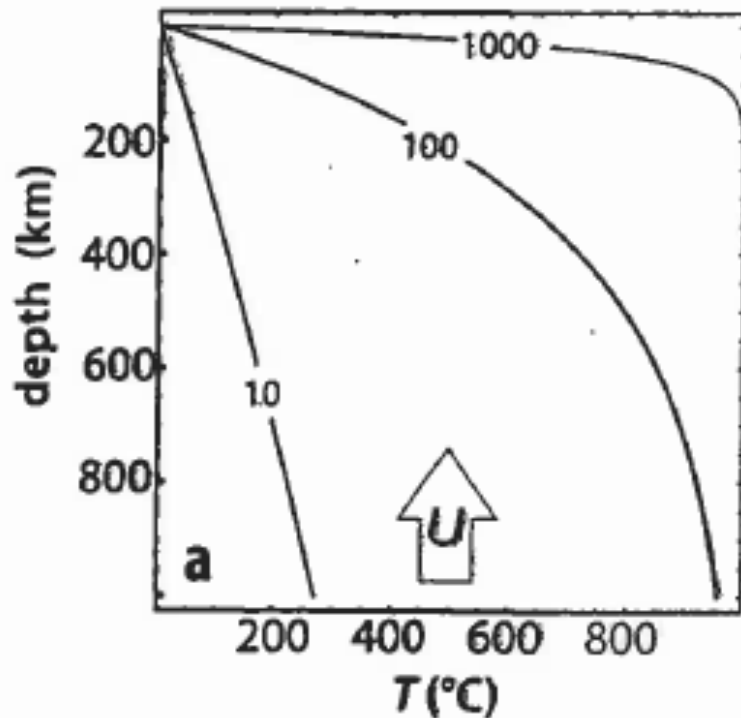
$$T_{z=0} = 0$$

$$T = T_L = 1000^{\circ}\text{C}$$

$$L = 100 \text{ km}$$

$$s = 1 \times 10^{-6} \text{ m}^2 \text{ s}^{-1}$$

Contours: advection (erosion) rates in m/Ma

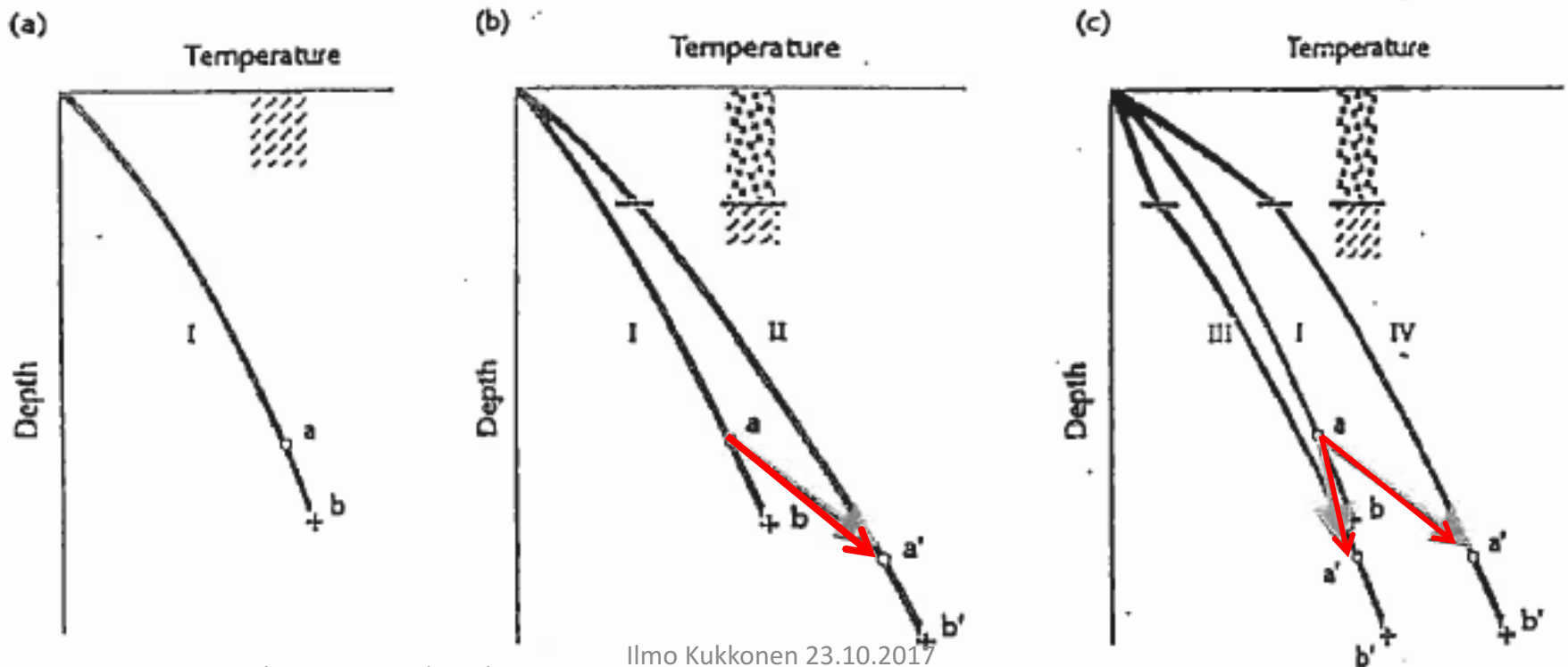


Stüwe 2002

Effect of sedimentary cover on temperature (schematically)

- (a) Comparison geotherm: Conditions before sedimentation
- (b) Sediment conductivity and heat production are the equal with the basement
- (c) Effect of thermal conductivity of sediment: curve IV: low conductivity, III: high conductivity

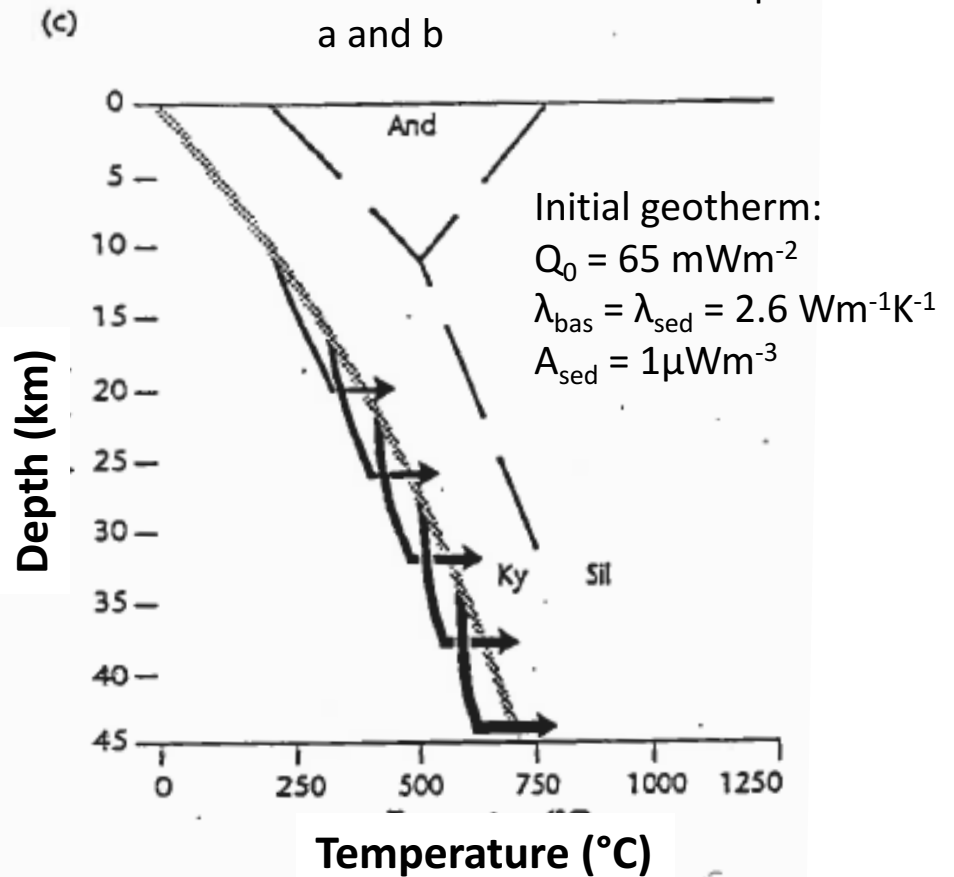
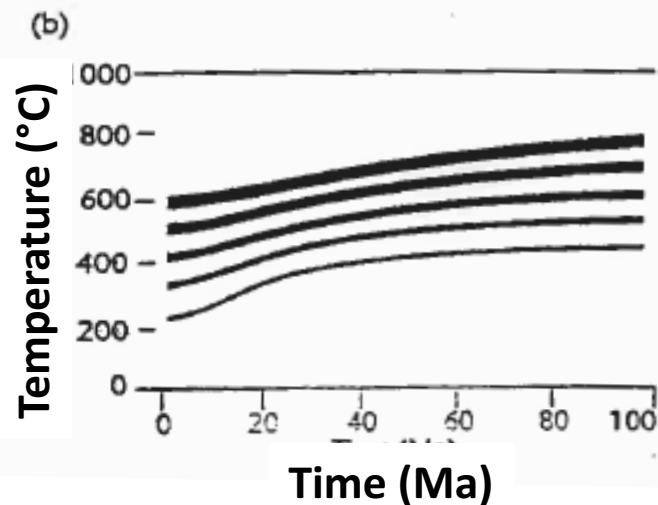
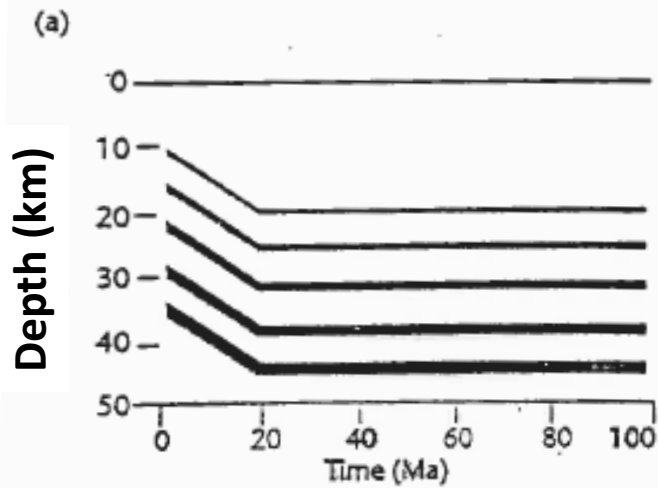
- a, b: original z-T conditions, a', b': new equilibrium conditions after sedimentation



Effect of sedimentation when time is taken into account

10 km of sedimentation and subsidence during 20 Ma

Thickness of arrows corresponds to the line thicknesses in panels in a and b



Chapman and Furlong 1992

Extension: "Pure shear" and "simple shear"

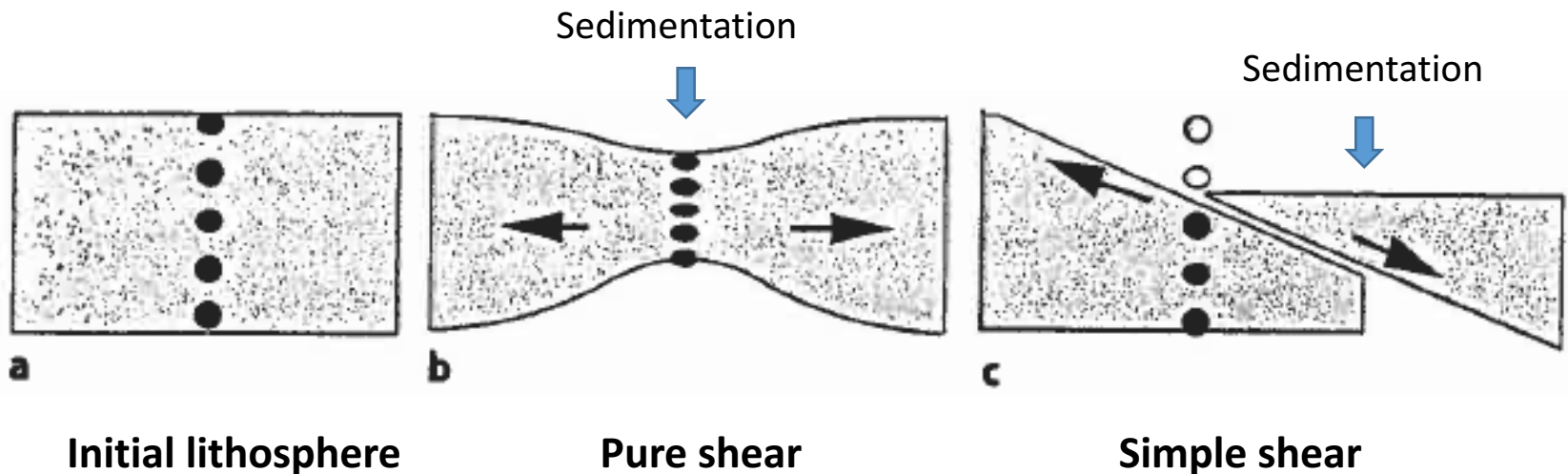
- Extension is one of the fundamental tectonic processes leading to formation of sedimentary basins and breaking up of continents

Pure shear (b): Lithosphere thins by extension

- After extension mid-crustal rocks do not outcrop at erosion level
- Sedimentation covers the extended part

Simple shear (c): Lithosphere thins by shearing (along a low-angle normal fault)

- Due to uplift high-grade rocks are exhumed to surface level

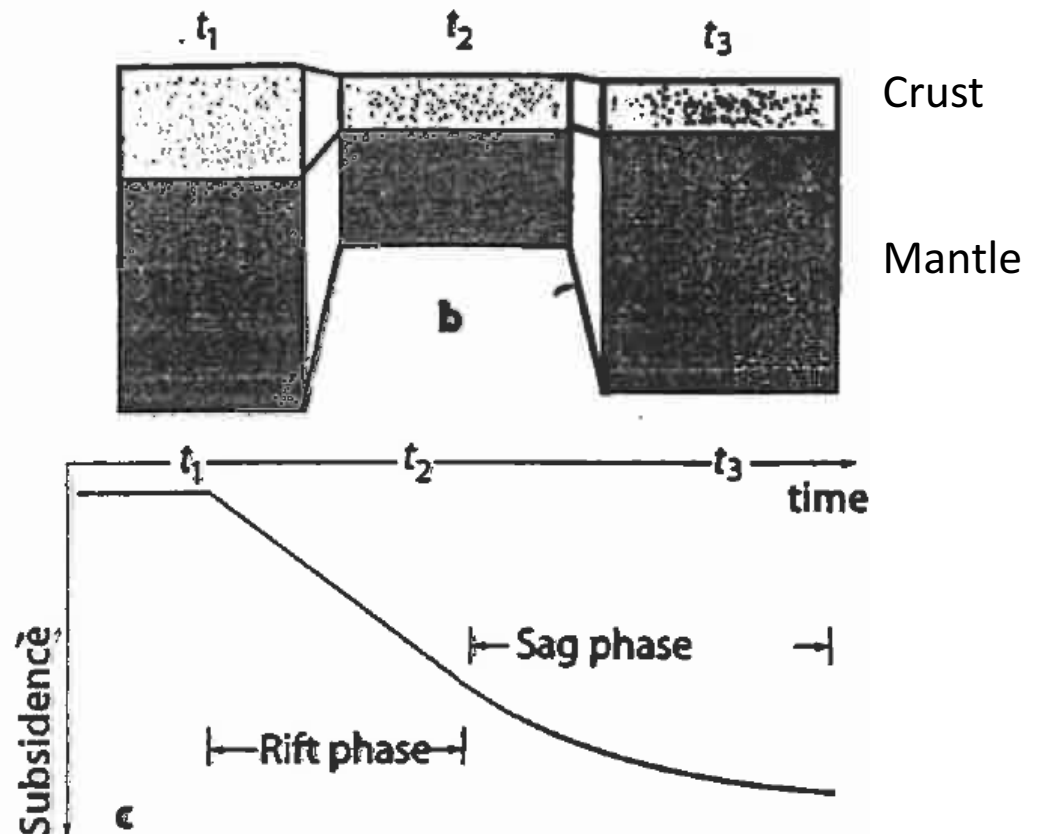
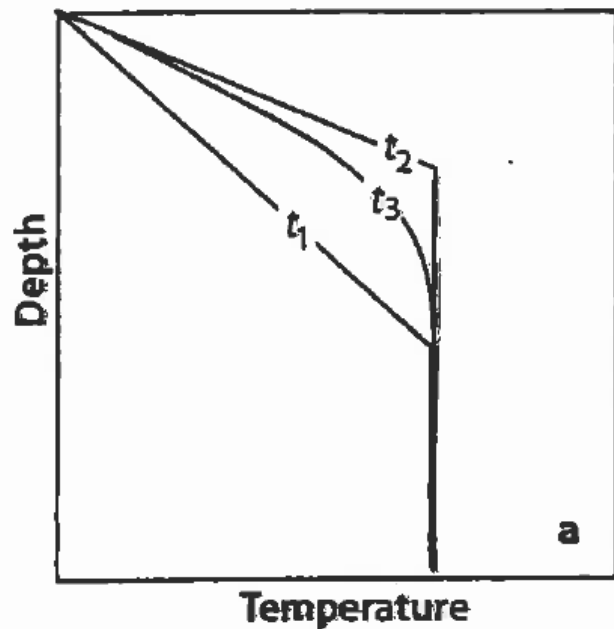


MacKenzie-type extension models

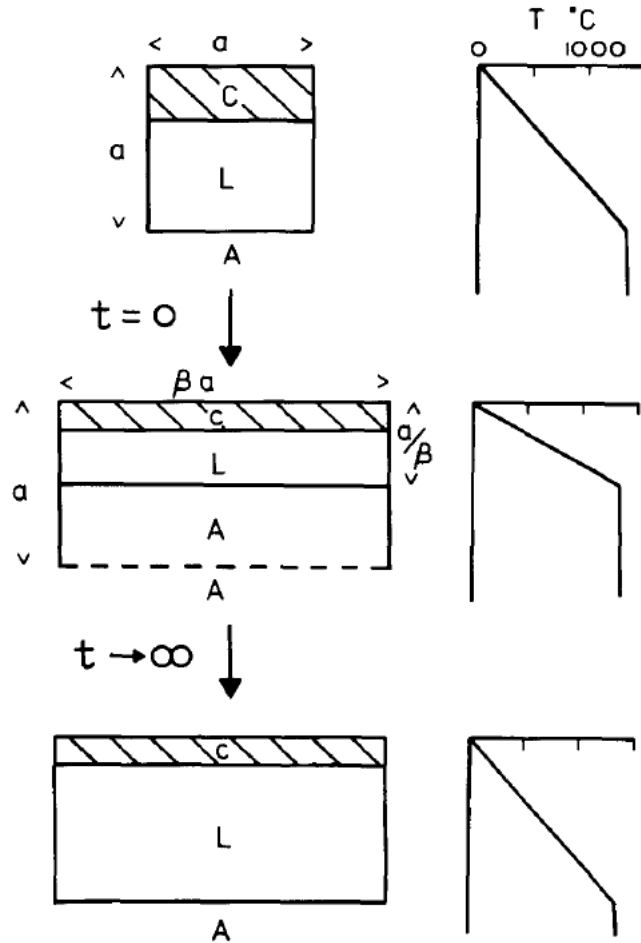
- Extension is **by pure shear** in MacKenzie models
- Extension is assumed to take place much faster than the thermal relaxation time of the lithosphere ($t = L^2/a$) (In the model extension takes place instantaneously)
- The extended part of lithosphere extends by a factor β
- Typically in intracontinental basins β is about 1-2
- In continental margin basins β ranges from about 1 on continental slopes onshore to 4...5 offshore
- The MacKenzie model (1978) has been widely used due to its simplicity, and there are many refinements of it in the subsequent literature
- Presently extension modeling is most often done with numerical models

Principles of the MacKenzie model

- Prior to onset of extension (t_1)
- At the end of the stretching phase (t_2)
- During subsequent thermal equilibration of the lithosphere (t_3)



Phases of the MacKenzie extension model



Initial equilibrium lithosphere

- Heat production is neglected in the model
- Crust and mantle have equal conductivities

Instantaneous extension by factor β

- Increase of geothermal gradient by factor β
- Upwelling of astenospheric material

Cooling and re-thickening of the lithosphere

- Thickening of the mantle part releases a transient pulse of heat
- With long times, lithosphere equilibrates again

Temperature of the lithosphere before extension :

$$T = T_0 + (T_L - T_0)(z / L) \quad (10.8)$$

And after extension :

$$T = T_0 + (T_L - T_0) \times (\beta z / L) \quad (10.9)$$

where

T_0 is surface temperature,

T_L is the temperature at the lower boundary of the lithosphere (asthenosphere temperature),

L is the thickness of the lithosphere before extension

β is the extension factor.

We assume for simplicity that $T_0 = 0$, then the temperature after extension is

$$T = T_L \times (\beta z / L) \quad (10.10)$$

After extension the geotherm finds a new equilibrium and heat is released due to re-thickening of the lithospheric mantle:

$$H = 0.5 \times L \times \rho c \times T_L (1 - 1/\beta) \quad [\text{J m}^{-2}] \quad (10.11)$$

Extension produces **a transient increase in heat flow.**

The temperature of the lithosphere after the extension can be obtained with the transient solution of a 1-dimensional layer (Carslaw and Jaeger, 1959):

$$T(z, t) = T_L \left(\frac{z}{L} \right) + T_L \sum_{n=1}^{\infty} \left[a_n \sin \left(\frac{n\pi z}{L} \right) \exp \left(-s \left(\frac{n\pi}{L} \right)^2 t \right) \right] \quad (10.12)$$

where s is diffusivity and the factors a_n are

$$a_n = \frac{2\beta}{(n\pi)^2} \sin \left(\frac{n\pi}{\beta} \right) \quad (10.13)$$

Heat flow at the surface after extension is :

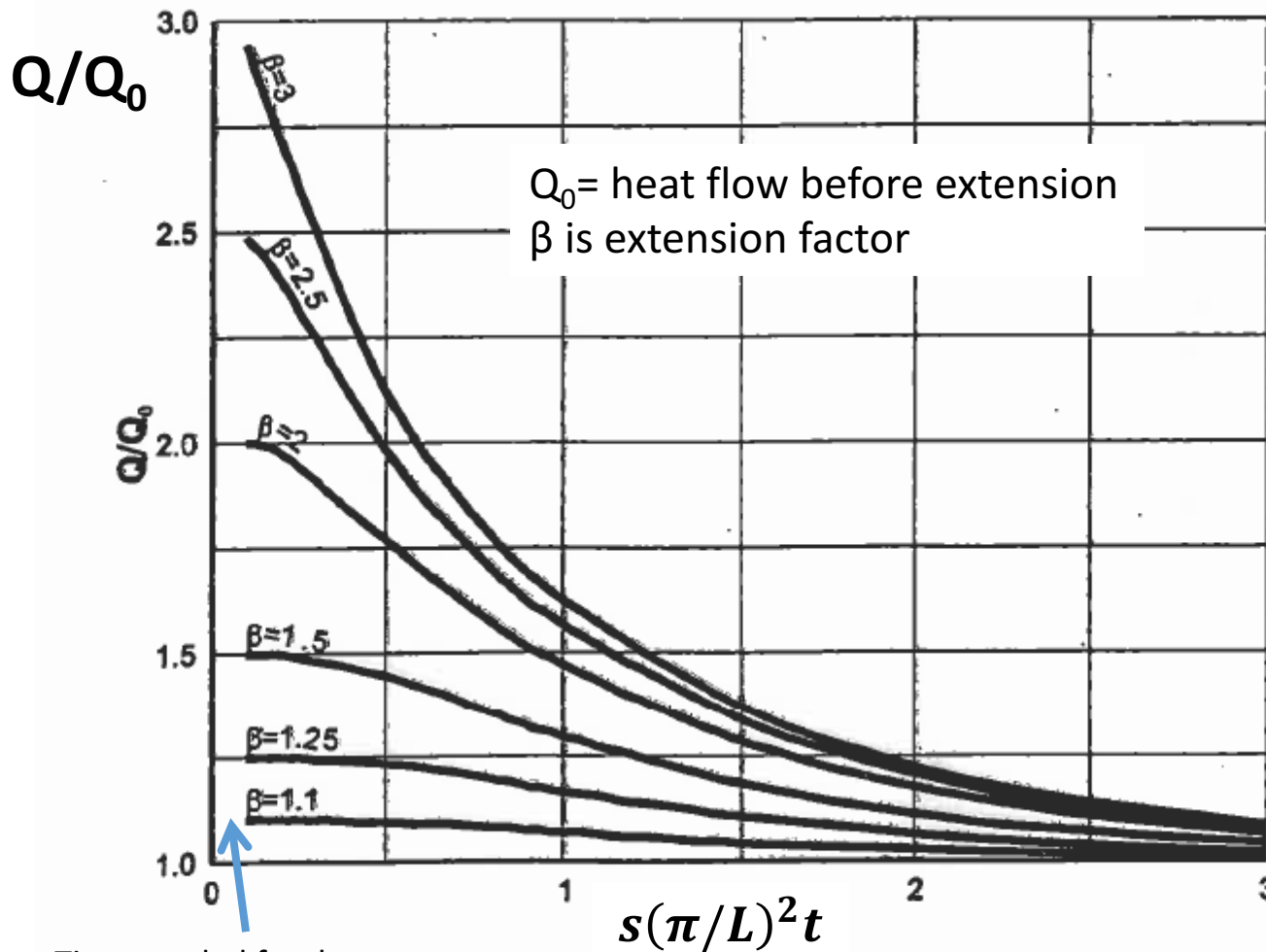
$$Q = \lambda \frac{T_L}{L} \left\{ 1 + 2 \sum_{n=1}^{\infty} \left[\frac{\beta}{n\pi} \sin \frac{n\pi}{\beta} \right] \exp \left(-s \left(\frac{n\pi}{L} \right)^2 \right) \right\} \quad (10.14)$$

- The heat flow equation is valid for times **longer than the characteristic time defined as**

$$\tau = \frac{L^2}{\pi^2 s} \quad (10.15)$$

- The heat flow evolution is shown in the figure on next page.

Change of heat flow due to extension



Q_0 = heat flow before extension
 β is extension factor

- Heat flow increases at maximum by factor β

Parameters of dimensionless time:

- L is thickness of lithosphere before extension
- s is diffusivity
- t is time

Time needed for the heat flow signal to penetrate the crust

Dimensionless time

Beardsmore and Cull 2001

The thinning of lithosphere due to extension produces

- **isostatic subsidence** of lithosphere (S_i)
- **uplift of asthenosphere.**
- The amount of subsidence depends on the amount of stretching, initial crustal thickness (t_c) and lithosphere thickness (L) and the densities of crust, lithospheric mantle and asthenosphere.
- The densities are affected by thermal contraction and expansion
- The isostatic subsidence (S_i) is obtained from

$$S_i = \left(1 - \frac{1}{\beta}\right) \frac{[t_c \rho_c + (L - t_c) \rho_m - L \rho_a]}{(\rho_w - \rho_a)} \quad (10.16)$$

where

$\rho_a = \rho_{m0}[1 - \alpha T_1]$ = density of the asthenosphere

$\rho_m = \rho_{m0}[1 - \alpha(T_0 + 0.5(T_L - T_0)(1 + t_c/L))]$ = density of the lithospheric mantle

$\rho_c = \rho_{c0}[1 - \alpha(T_0 + 0.5(T_L - T_0)(t_c/L))]$ = density of crust

ρ_w = density of water filling the extension basin

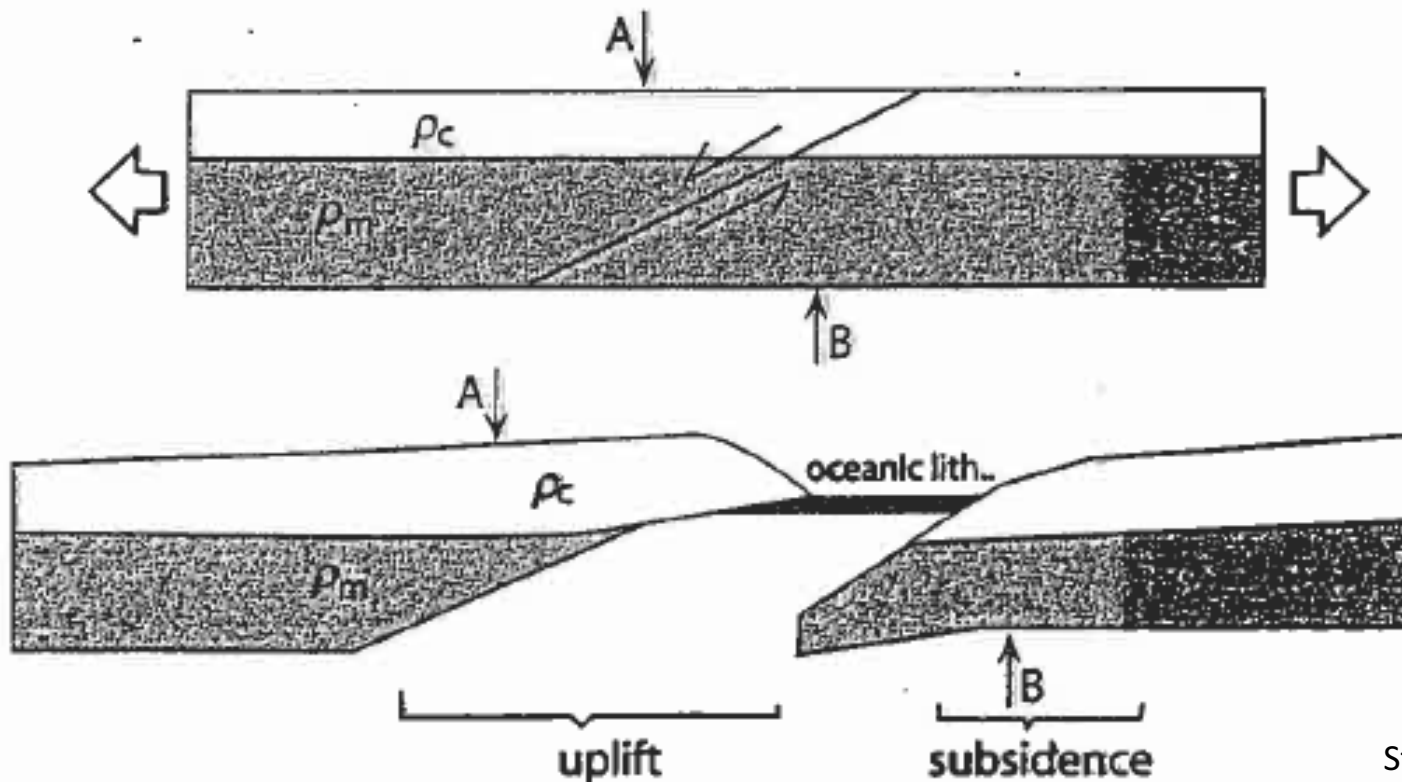
T_0 = surface temperature

α = thermal expansion coefficient of rock

ρ_{m0} ja ρ_{c0} are the densities of mantle and crust at reference temperature (0°C)

Extension by normal faulting (simple shear)

- **Low-angle normal fault** intersects the whole lithosphere
- Development of **passive continental margins**
- At location A extension **decreased the thickness of the mantle part** of lithosphere
- At B extension **decreased the thickness of the crust**
- As a result there is **isostatic uplift** the of the passive margin of A and **subsidence** at B

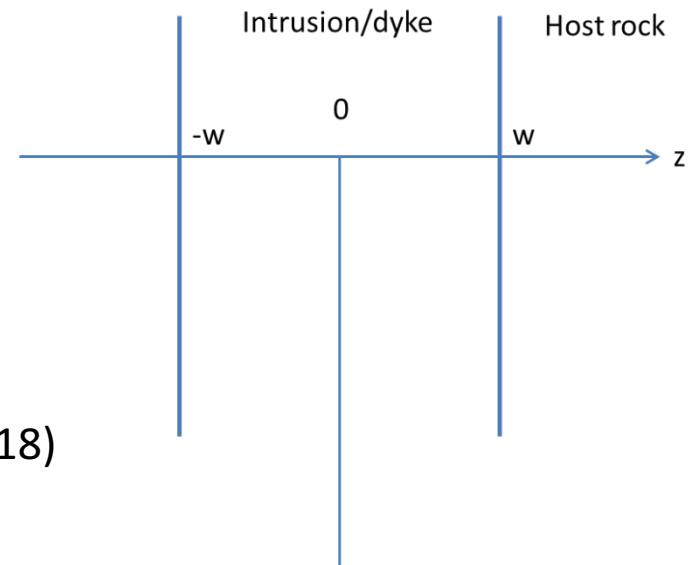


Stüwe 2002

Thermal effects of a plate-form intrusion

- We assume the intrusion to be an infinitely long plate (a sill or dyke) located at a sufficiently long distance from the surface (full-space medium)
- Heat conduction equation without heat production :

$$s \frac{\partial^2 T}{\partial z^2} = \frac{\partial T}{\partial t} \quad (10.17)$$



- Intrusion is located at $-w \leq z \leq +w$.
- Boundary condition of the initial state :
 $T = T_0$, when $t = 0$, $-w \leq z \leq +w$
 $T = T$, when $t = 0$, $|x| > w$

$$(10.18)$$

$$\Delta T_0 = T_0 - T, \text{ kun } t = 0$$

The solution is once again provided by Carslaw and Jaeger (1959)

$$\Delta T(z, t) = \frac{\Delta T_0}{2} \left[\operatorname{erfc} \frac{(w - z)}{2\sqrt{st}} + \operatorname{erfc} \frac{(w + z)}{2\sqrt{st}} \right] \quad (10.19)$$

Example of a cooling dyke.

The dyke is 2 m thick, $w = 1$ m, $T_0 = 1000$ °C, $T = 0$, $s = 1 \cdot 10^{-6}$ m²s⁻¹ .

Temperatures at the centre of the dyke :

$$T(0, 1 \text{ week}) = 640^\circ\text{C}$$

$$T(0, 1 \text{ month}) = 340^\circ\text{C}$$

$$T(0, 1 \text{ year}) = 100^\circ\text{C}$$

→dykes cool very rapidly!

There are rules of thumb for the temperature at the center of the dyke :

$$\Delta T \approx \frac{\Delta T_0}{2}, \text{ when } t = \frac{w^2}{s} \quad (10.20)$$

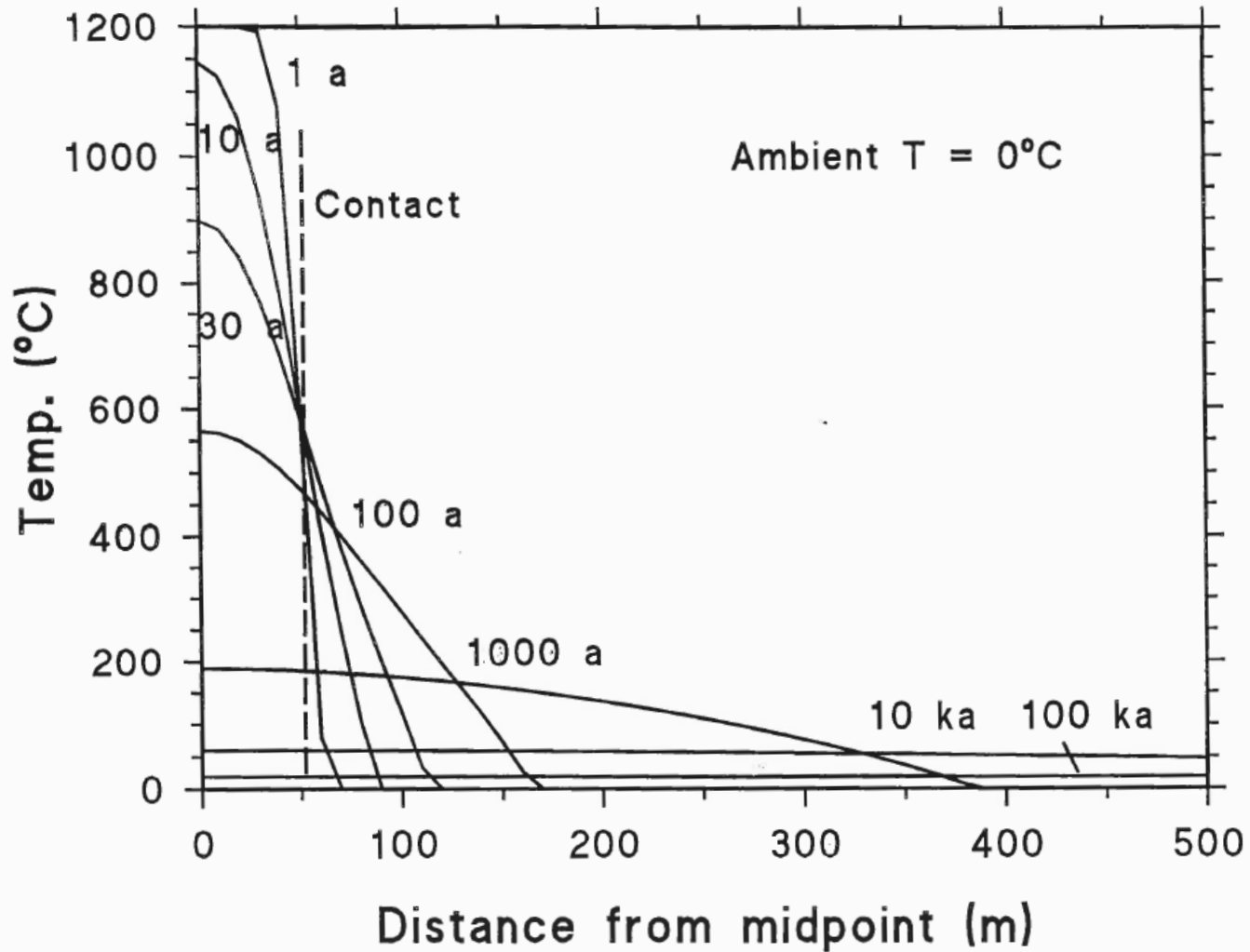
$$\Delta T \approx \frac{\Delta T_0}{4}, \text{ when } t = \frac{5w^2}{s} \quad (10.21)$$

For the area **outside the dyke** there are the following approximations :

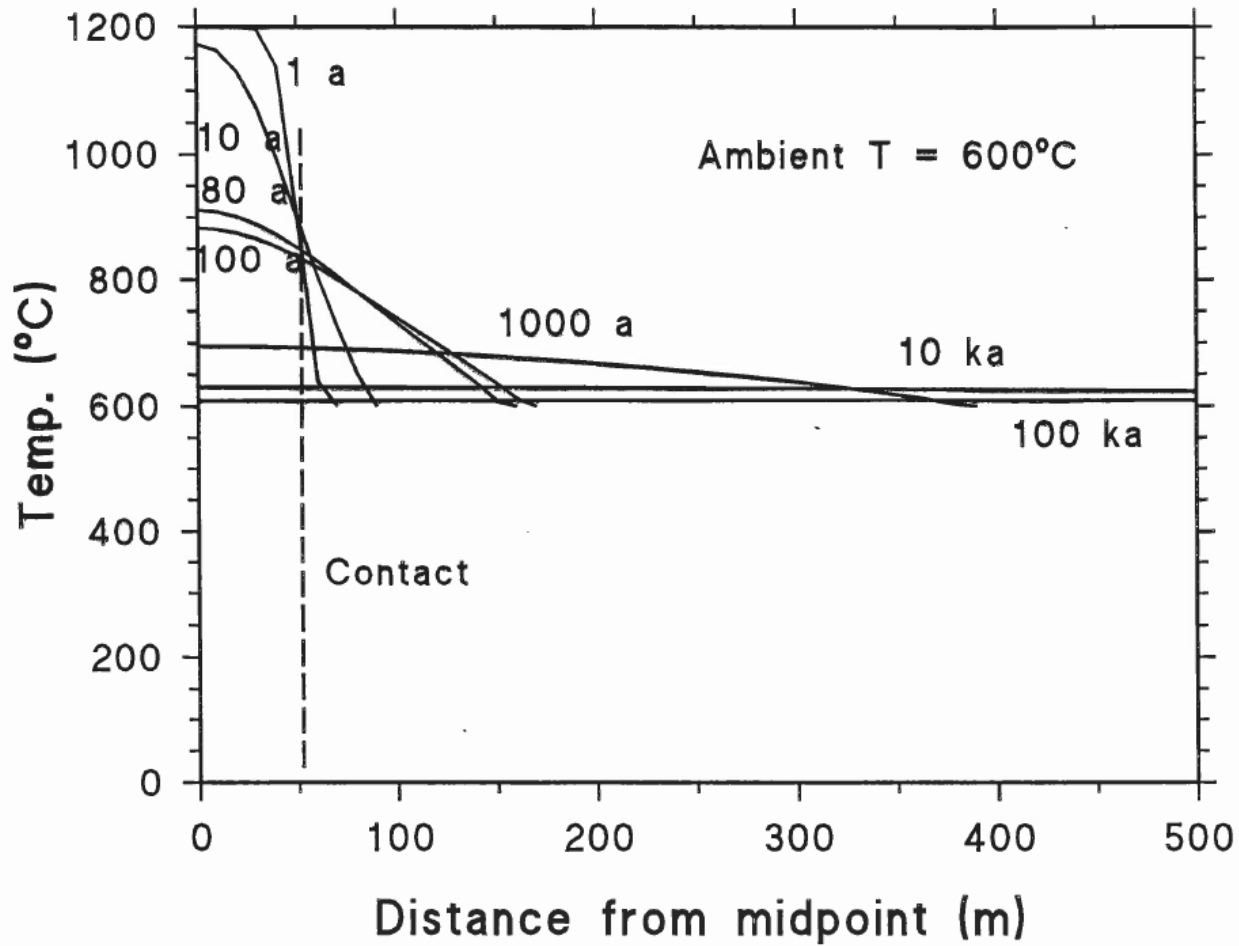
- Temperature maximum reached at $2w$:
$$\Delta T(2w) \approx \frac{\Delta T_0}{4} \quad (10.22)$$

- Temperature maximum reached at $w + w/4$:
$$\Delta T(w + w/4) \approx \frac{\Delta T_0}{2} \quad (10.23)$$

Cooling of a dyke near surface

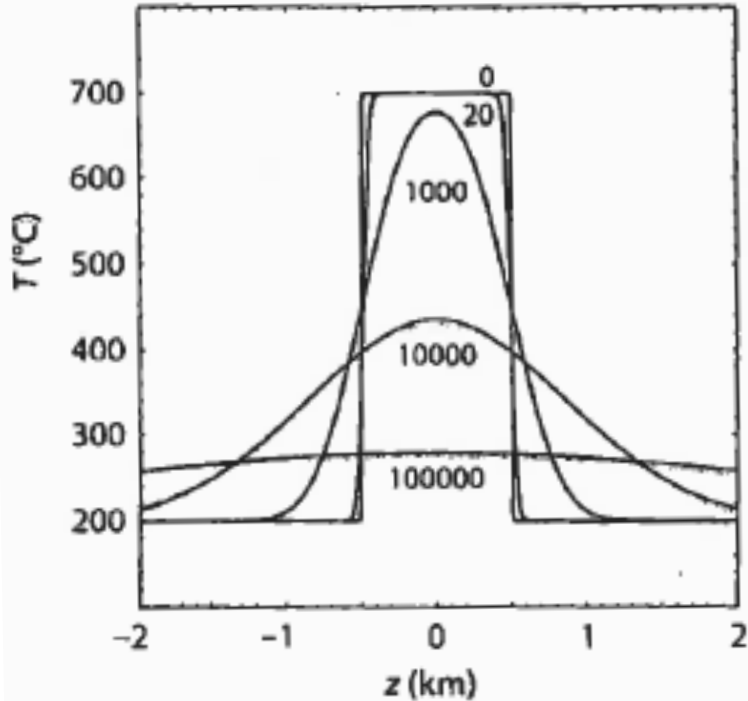


Cooling of a dyke in lower crust



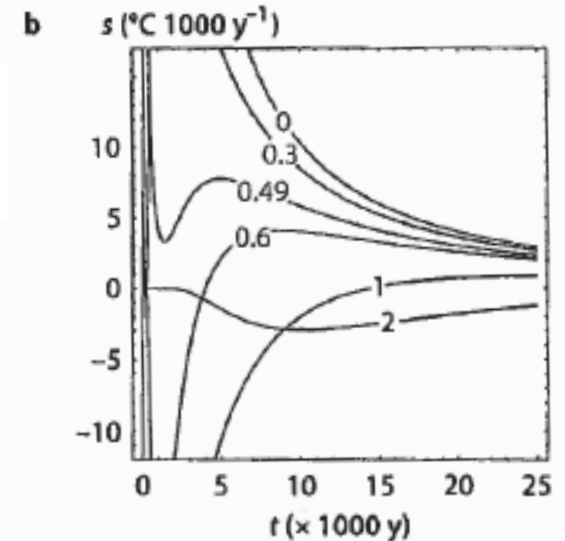
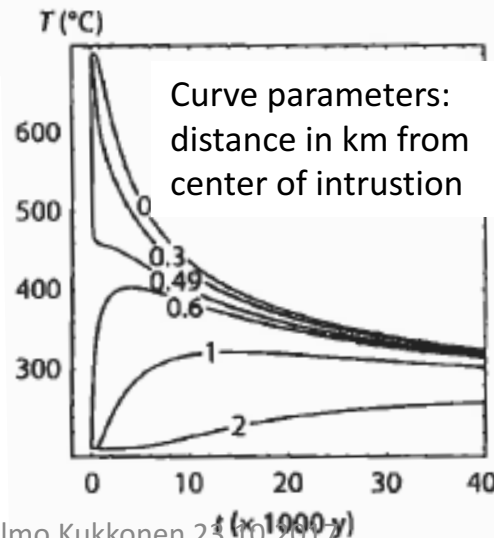
Examples of models of cooling intrusions

Stüwe 2002

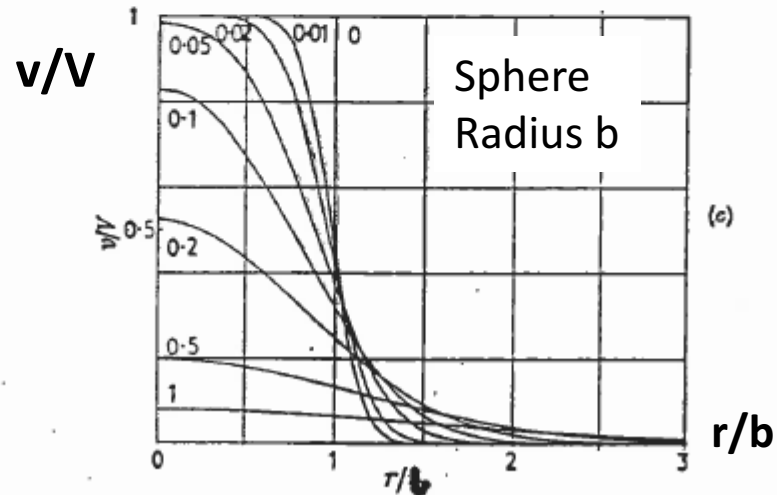
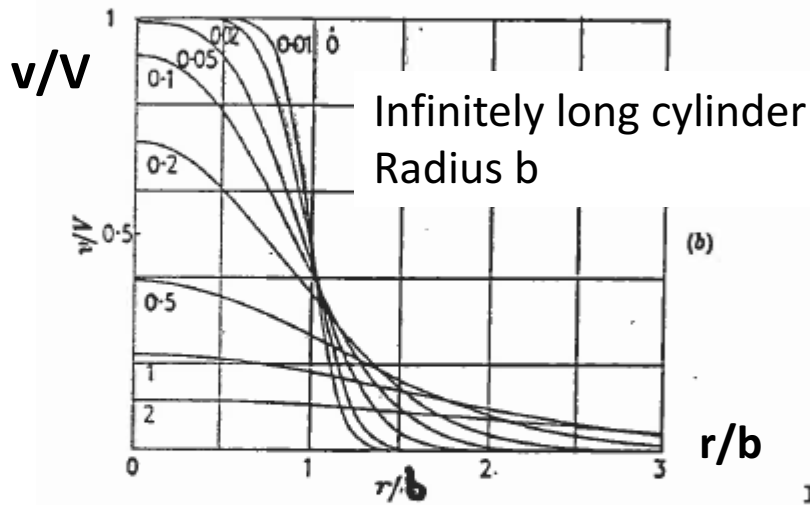
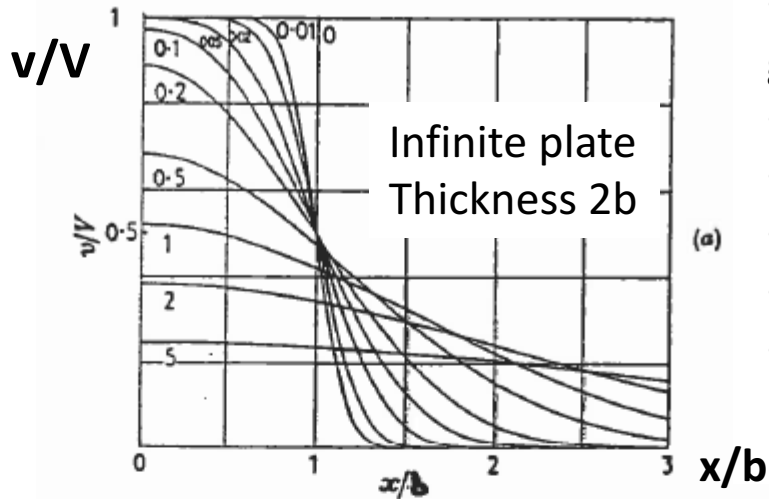


- 1 km thick intrusion (layer) :
- Cooling time in years
- Conductive model
- Calculated from the dyke model

Host rock temperature and cooling rate



Cooling of a plate, cylinder and sphere



- Dimensionless variables have been used in these graphs
- Initial temperature of body is V
- Initial temperature of the surrounding medium is zero
- Temperature is shown scaled as v/V
- Dimensions x/b , r/b or r/b
- The curve parameter is the Fourier number $F = st/b^2$

FIG. 4. Temperatures in an infinite region of which part is initially at constant temperature V and the remainder at zero: (a) the region $|x| < b$ initially at V ; (b) the interior of the cylinder $r = b$ initially at V ; (c) the interior of the sphere $r = b$ initially at V . In all cases the numbers on the curves are the values of xt/a^2 .

Carslaw and Jaeger, 1959

In the C & J figure (plate-cylinder-sphere) the curve parameter is the **Fourier number**

$$F = st/b^2 \quad (10.23)$$

where b is dyke thickness, radius of cylinder or radius of sphere

Example, let's assume a dyke :

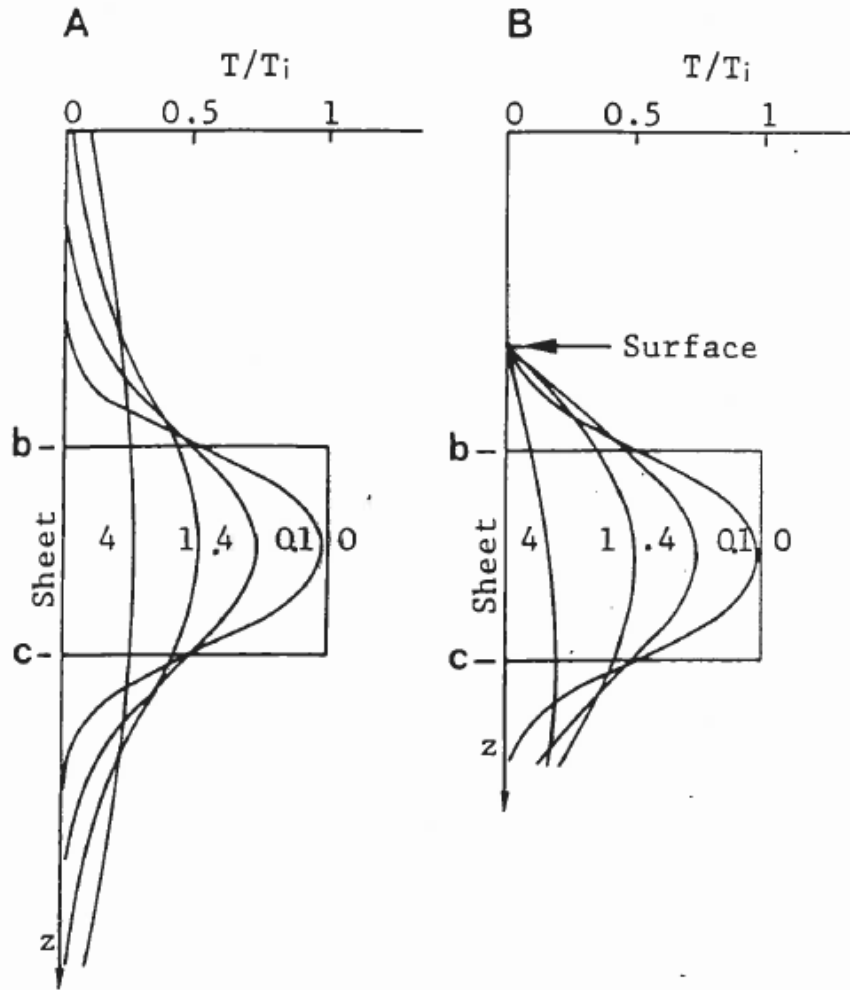
Thickness 2 km, initial temperature 1000 °C above host rock, $s = 1 \cdot 10^{-6} \text{ m}^2\text{s}^{-1}$

The Curve'5' corresponds to a time of about 160 000 years (dyke is quite cool already)

Note! On using conductive plate models in geological applications:

- The requirement of the distance from surface means a **(homogeneous) full-space** medium
- Moreover, the **latent heat of melt** has not been taken into account

Cooling dyke: Difference between half-space and full-space media



A: dyke in full-space medium

B: dyke in half-space medium close to surface

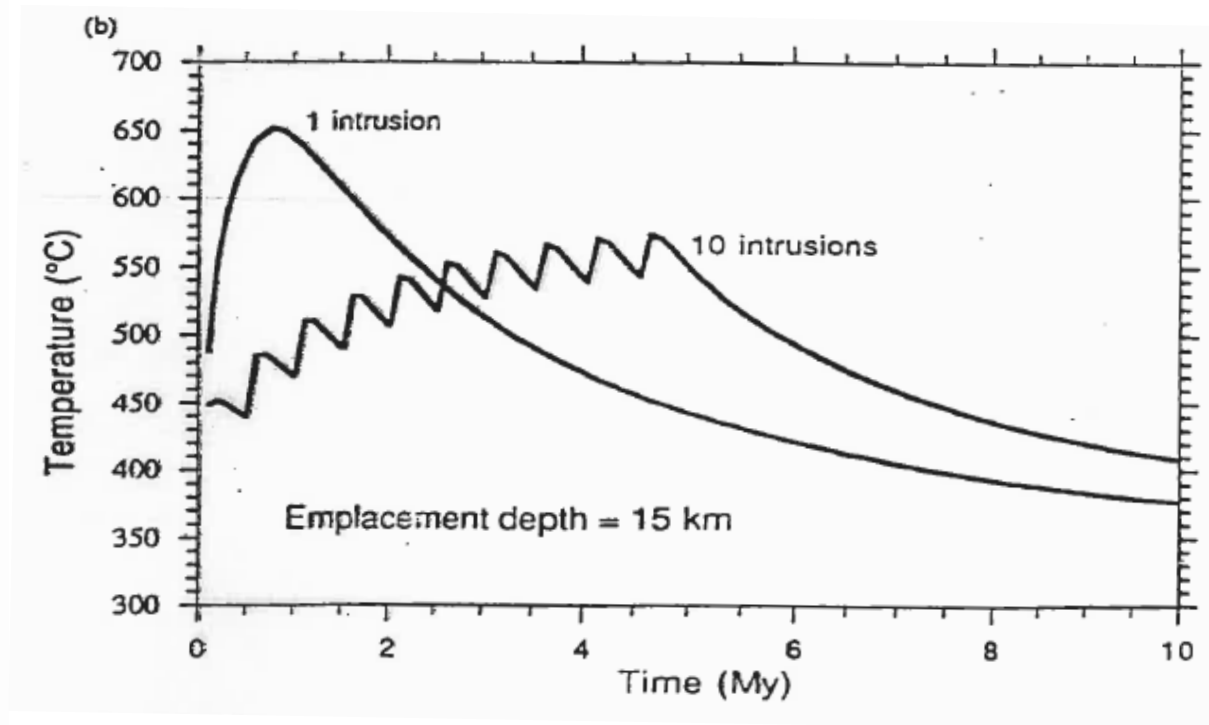
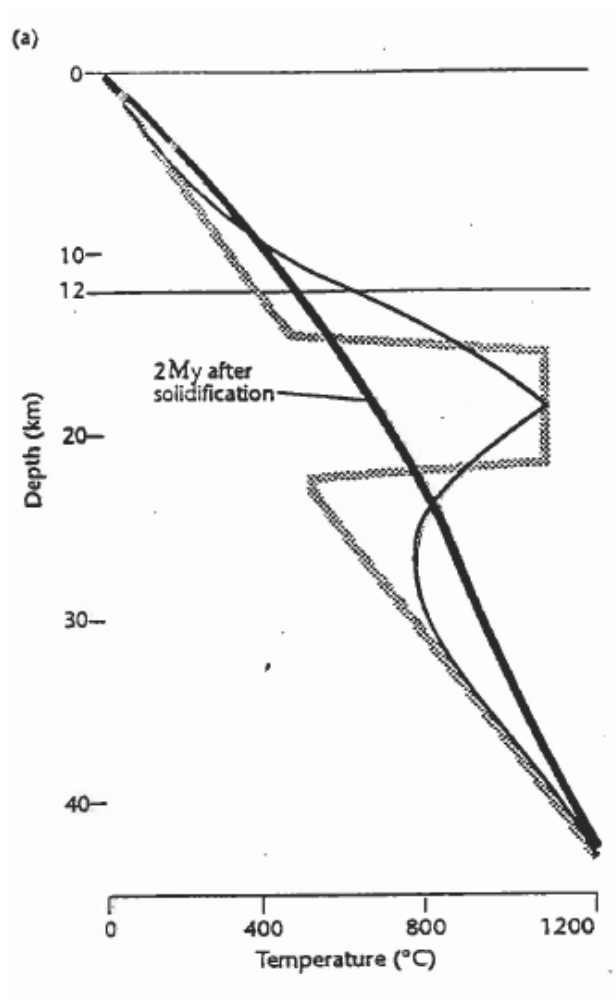
Curve parameter is the Fourier number

- The proximity of the surface kept at a constant temperature decreases the temperatures above the dyke and modifies them inside the dyke

Numerical modeling of thermal effect of intrusions

(a) 7.5 km thick sill intrudes at 15 km depth

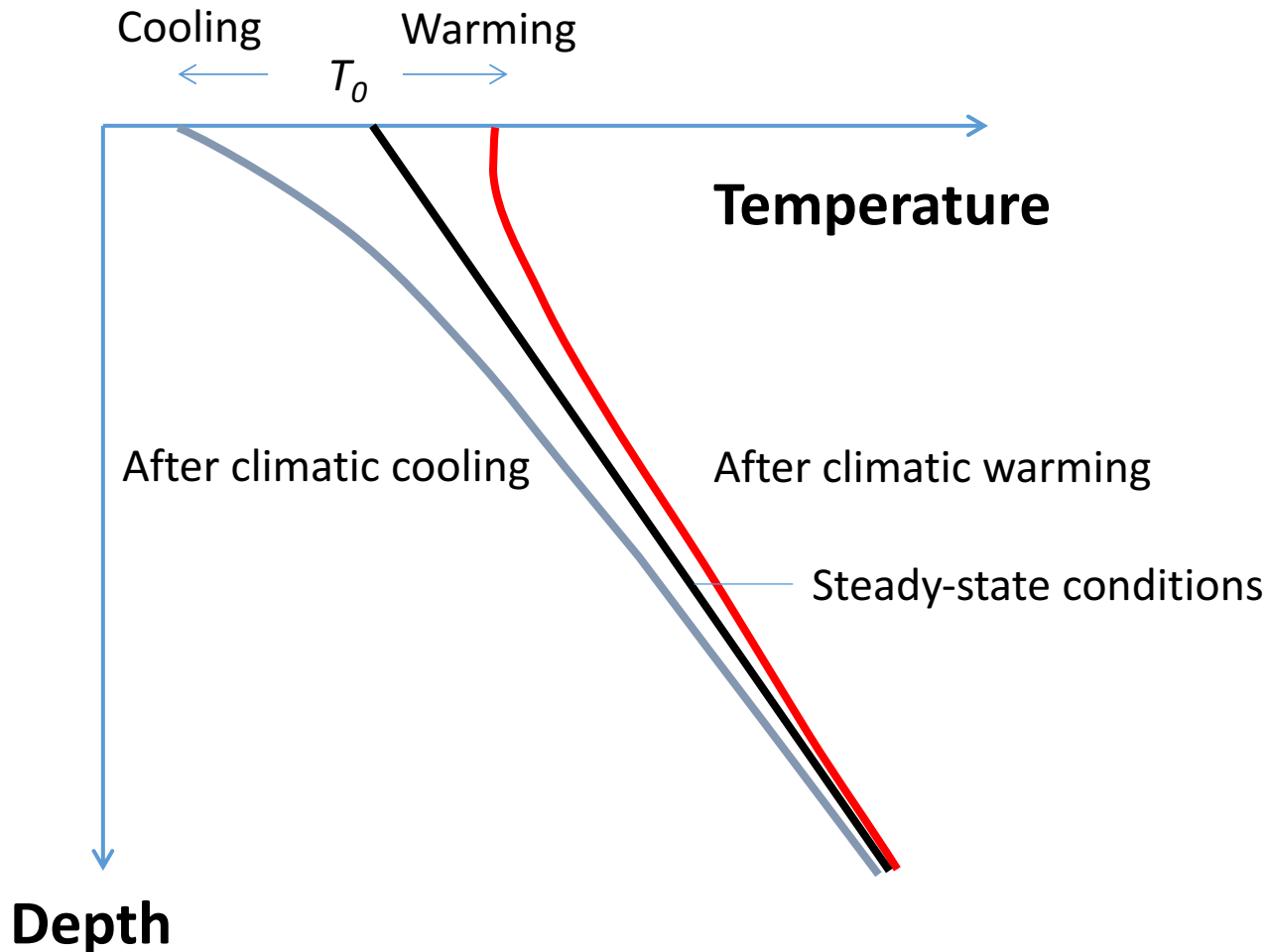
(b) Temperature at 12 km, sill is formed with one intrusion pulse of magma, or in 10 pulses



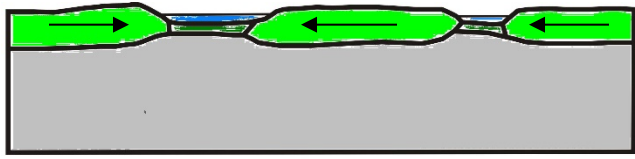
Chapman and Furlong 1992

Paleoclimatic effects on subsurface temperatures

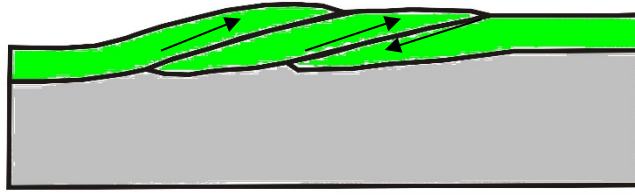
- Variations in ground surface temperature diffuse downward and attenuate in amplitude
- Temperatures are transient and do not represent steady-state conditions



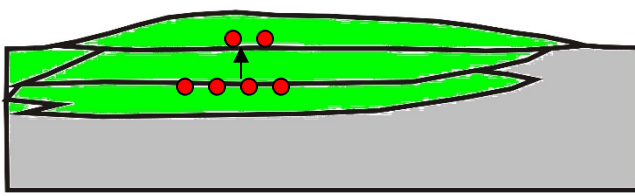
Building mountains by collision and imbricating crustal blocks



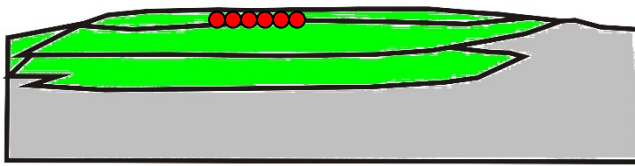
Before collision



Collision and thrusting
< 10-25 Ma



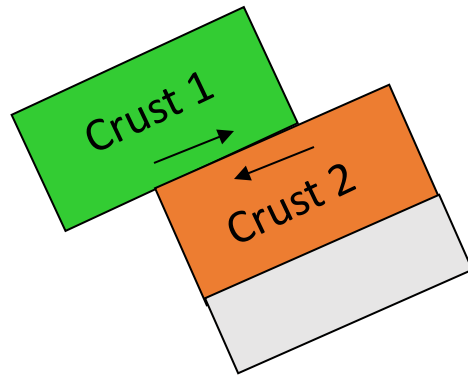
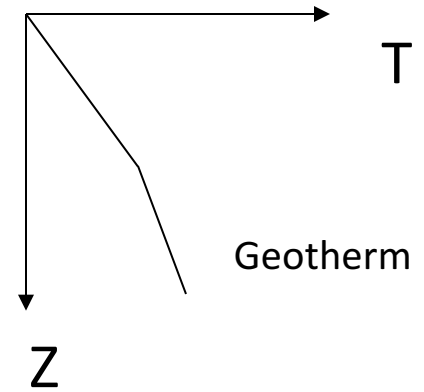
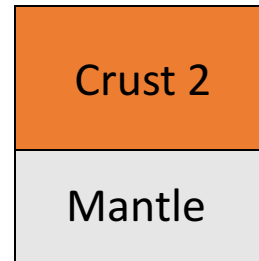
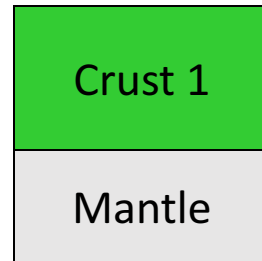
Thickened crust;
heating of stack, uplift erosion begins
Partial melting in middle/lower crust
10-50 Ma



Uplift, continued erosion, cooling
50-300 Ma

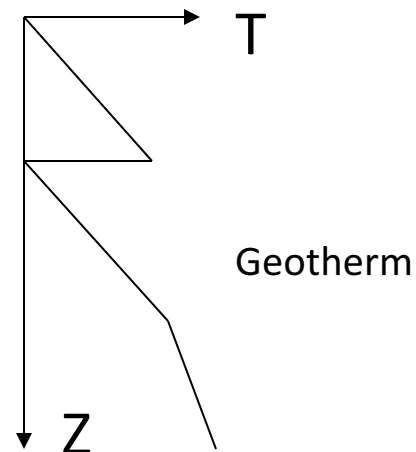
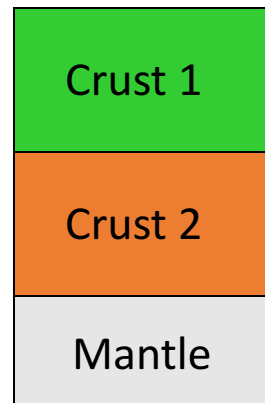
Principles of conductive thermal modelling of crustal stacking

**Situation
before collision**



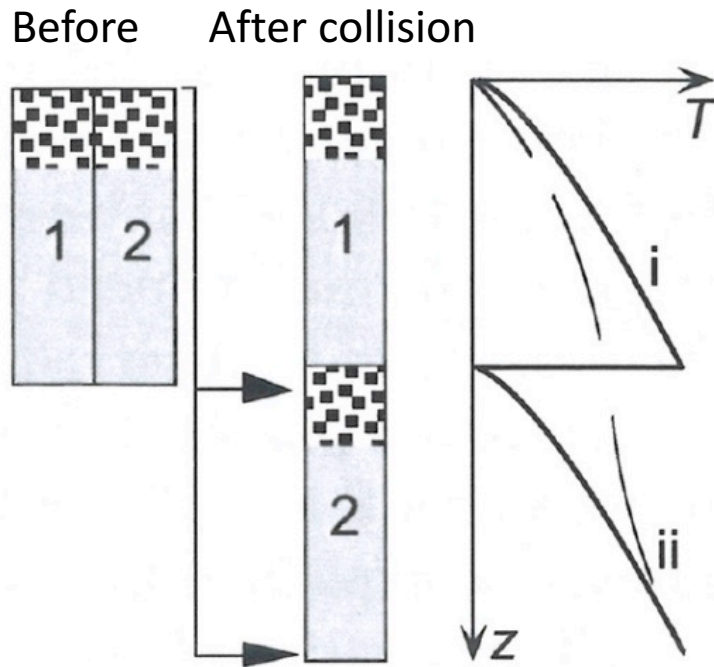
Collision and stacking

**Stack
t = 0 Ma**



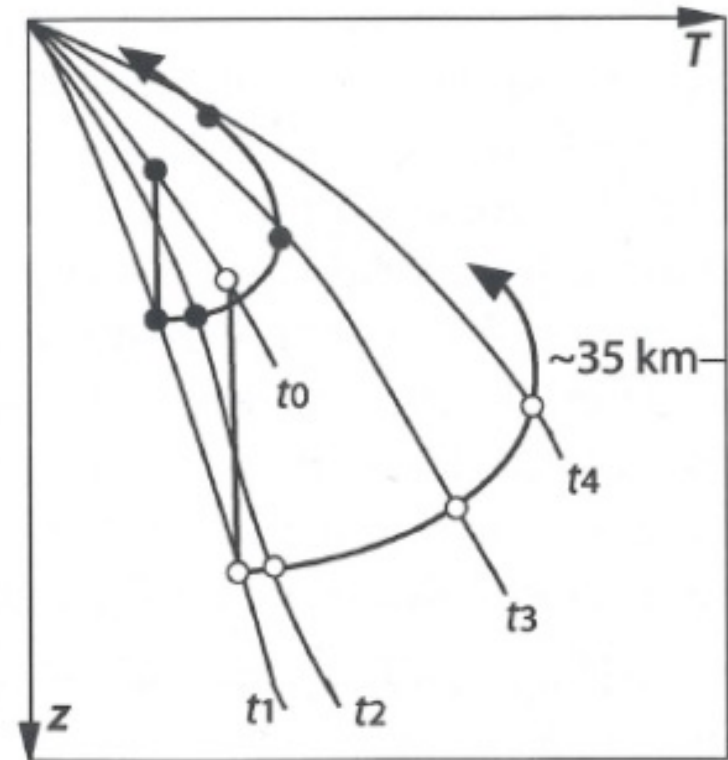
Temperature effects of crustal thickening

Initial situation



Temperature-depth-time plot

t_0 initial geotherm at time of collision
 t_0, t_1, t_2, t_3, t_4 geotherms at later times



Low-T thermochronology in Fennoscandia

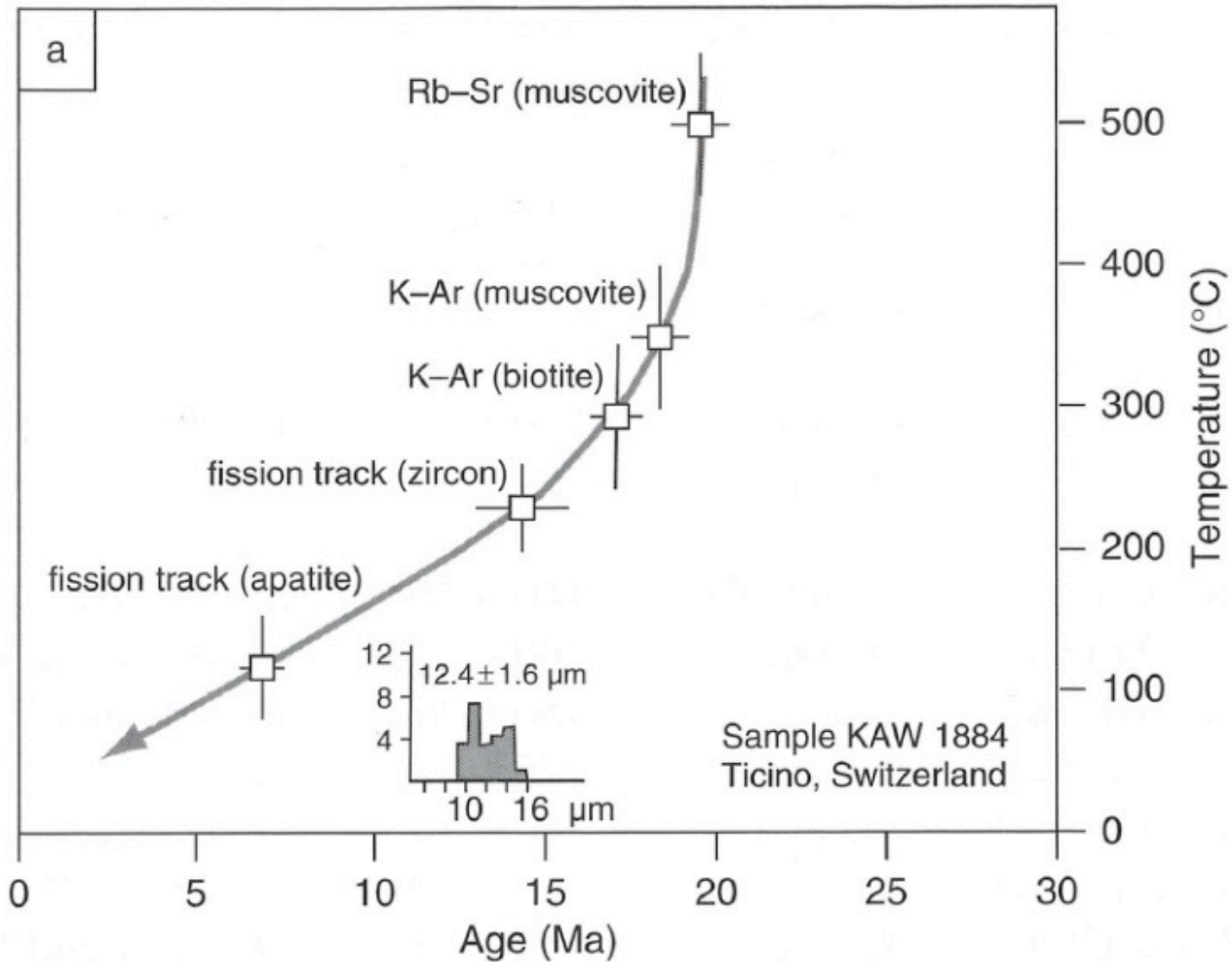
- Thermochrometers in general
- Mesoproterozoic - Phanerozoic geological history of Fennoscandia
- Apatite fission track results in Fennoscandia
- Geologically recent uplift and erosion – the Eridanos river system

Closure temperatures of common thermochronometers

Table 1.1. *Estimated closure temperatures for some commonly used thermochronometers*

Method	Mineral	Closure Temperature (°C)	Reference
K–Ar	Hornblende	500 ± 50	Harrison (1981)
K–Ar	Muscovite	350 ± 50	Hames and Bowring (1994)
K–Ar	Biotite	300 ± 50	Harrison <i>et al.</i> (1985)
K–Ar	K-feldspar	150 – 350	Lovera <i>et al.</i> (1989)
(U–Th)/He	Zircon	200 – 230	Reiners <i>et al.</i> (2002)
(U–Th)/He	Titanite	150 – 200	Reiners and Farley (1999)
(U–Th)/He	Apatite	75 ± 5	Wolf <i>et al.</i> (1998)
Fission track	Zircon	240 ± 20	Brandon <i>et al.</i> (1998)
Fission track	Titanite	265 – 310	Coyle and Wagner (1998)
Fission track	Apatite	110 ± 10	Gleadow and Duddy (1981)

Example: Applying several thermochronometers on a single sample from Swiss Alps



Geological evolution of Fennoscandia – from Archaean to Phanerozoic

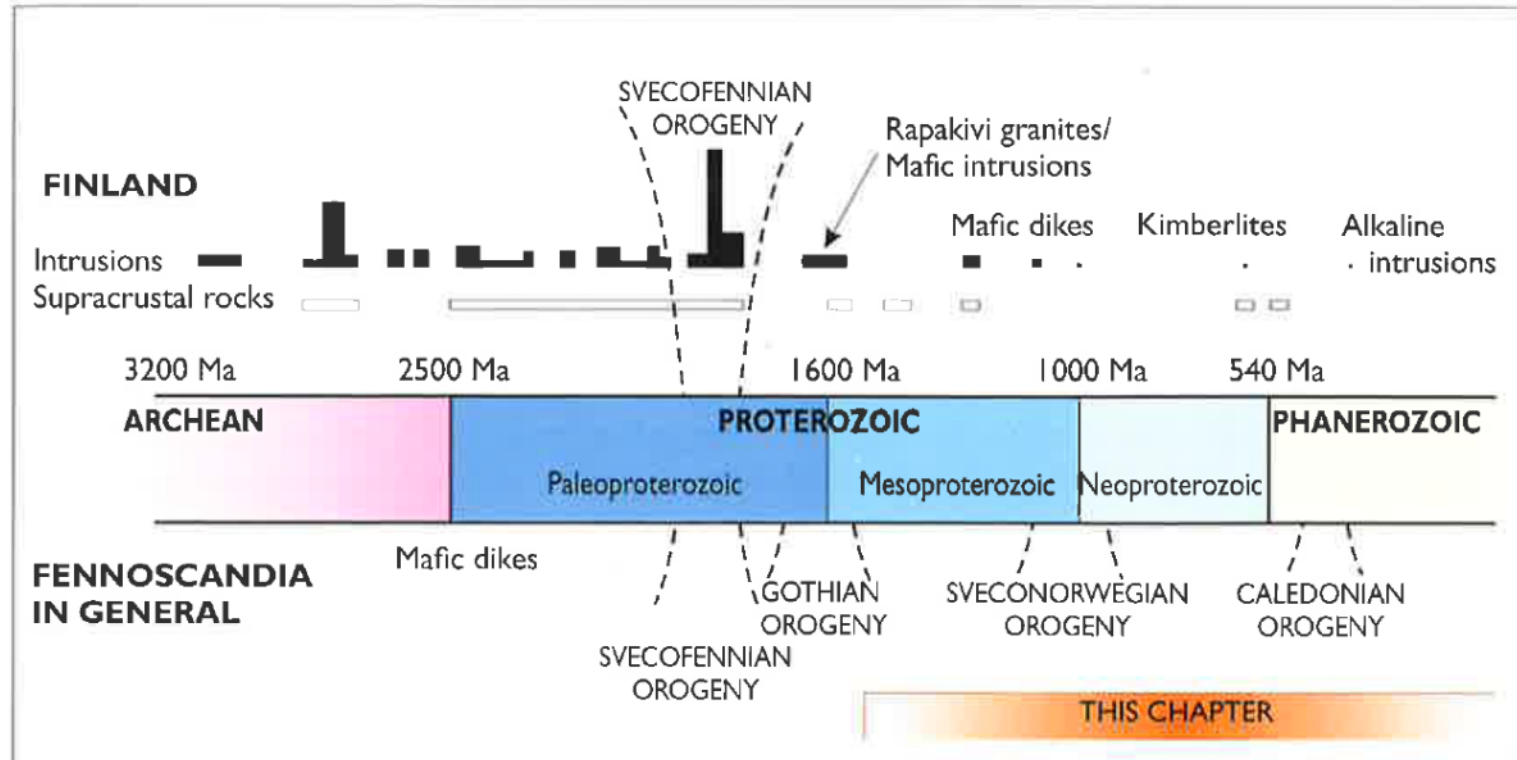
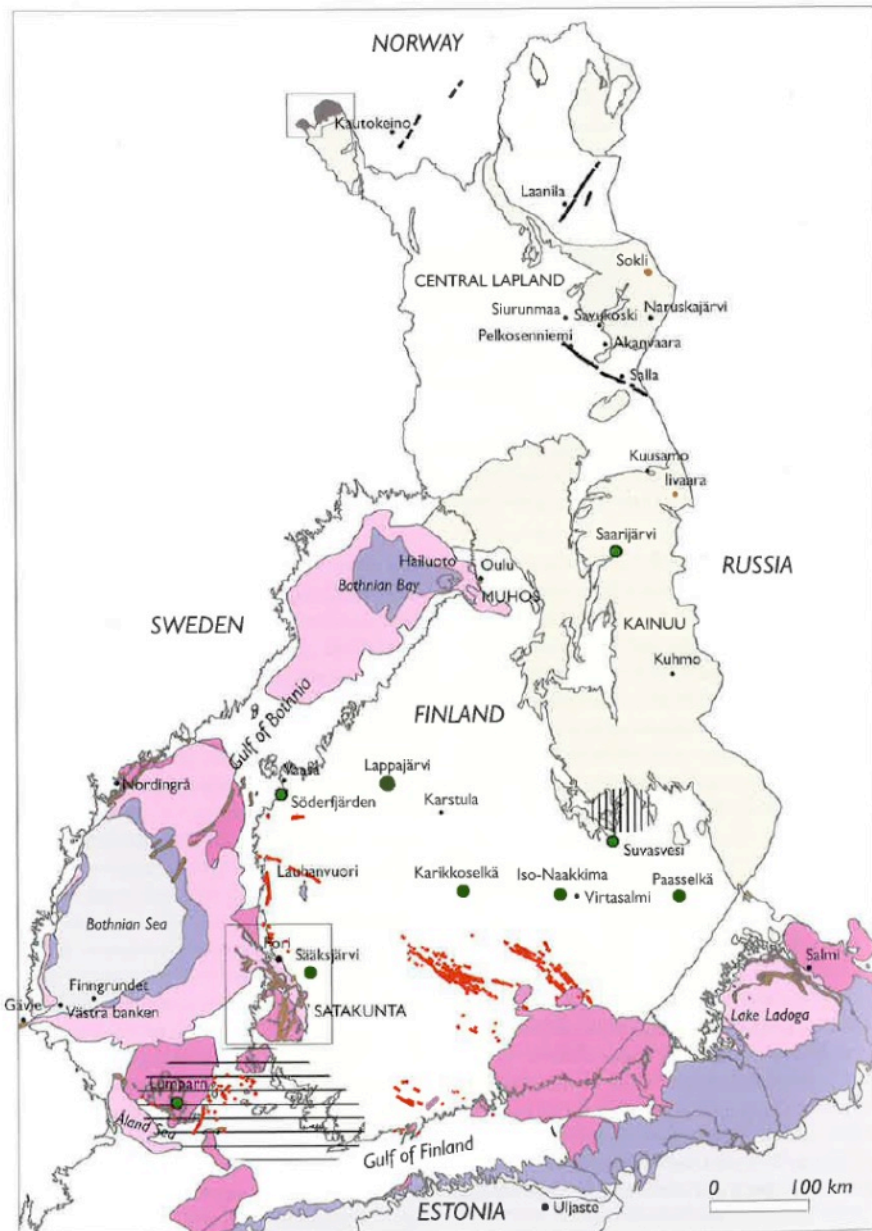
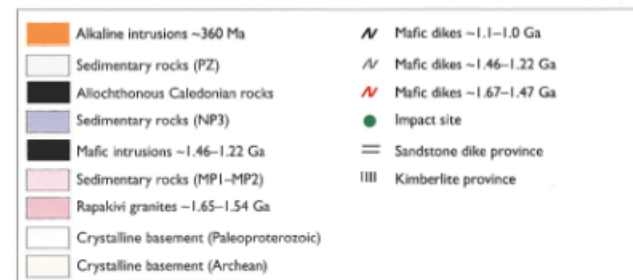


Fig. 13.1. Geological time scale with a sketch diagram of igneous activity and the presence of supracrustal rocks. Major orogenic events are also indicated.



Rämö & Kohonen, 2005



Mesoproterozoic to Cambrian sedimentary rocks and mafic dyke swarms

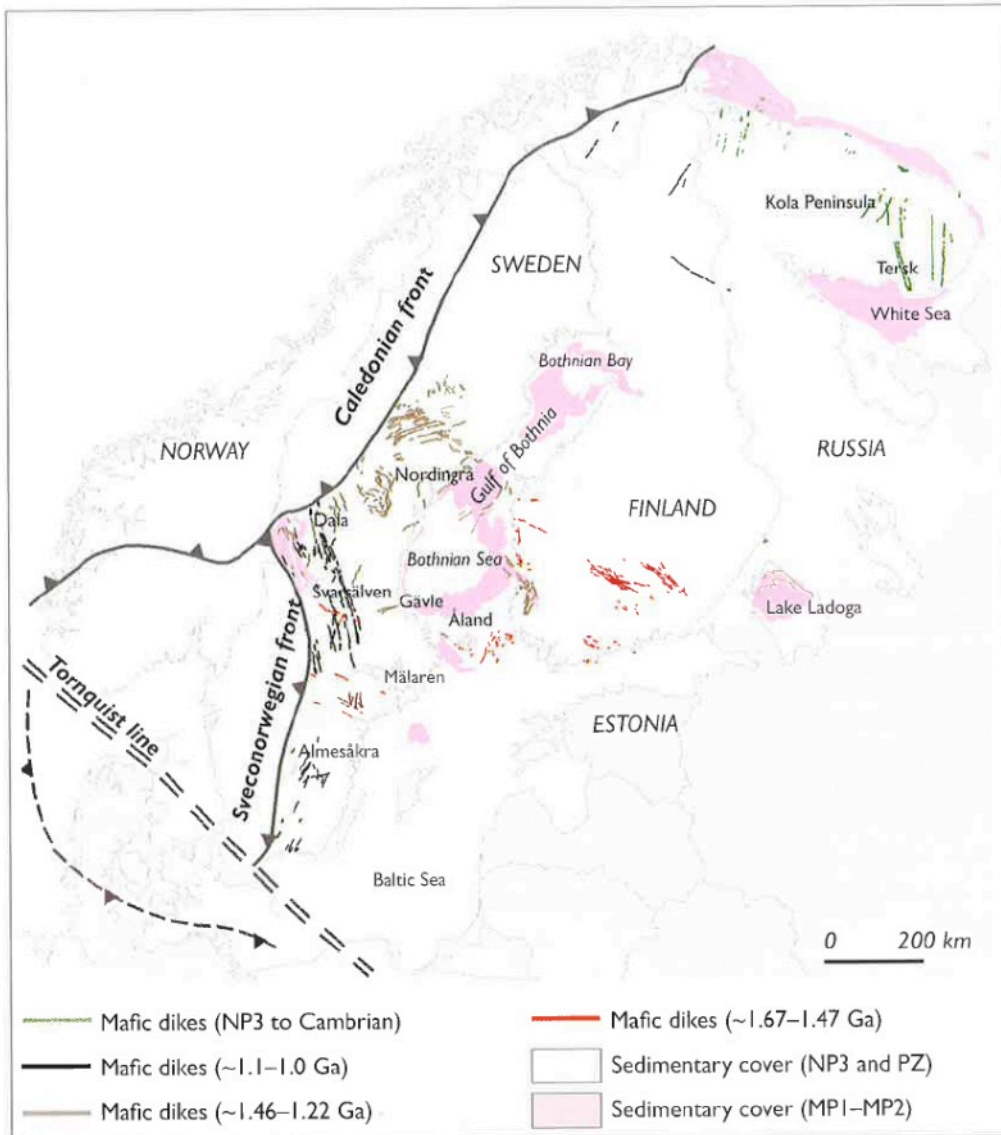


Fig. 13.3. Distribution of Mesoproterozoic to Cambrian sedimentary rocks and mafic dyke swarms in the central Fennoscandian Shield to the east of Sveconorwegian and Caledonian tectonic fronts. Dikes and other rock units simplified from Koistinen et al. (2001) and Mertanen et al. (1996a).

Rämö & Kohonen, 2005

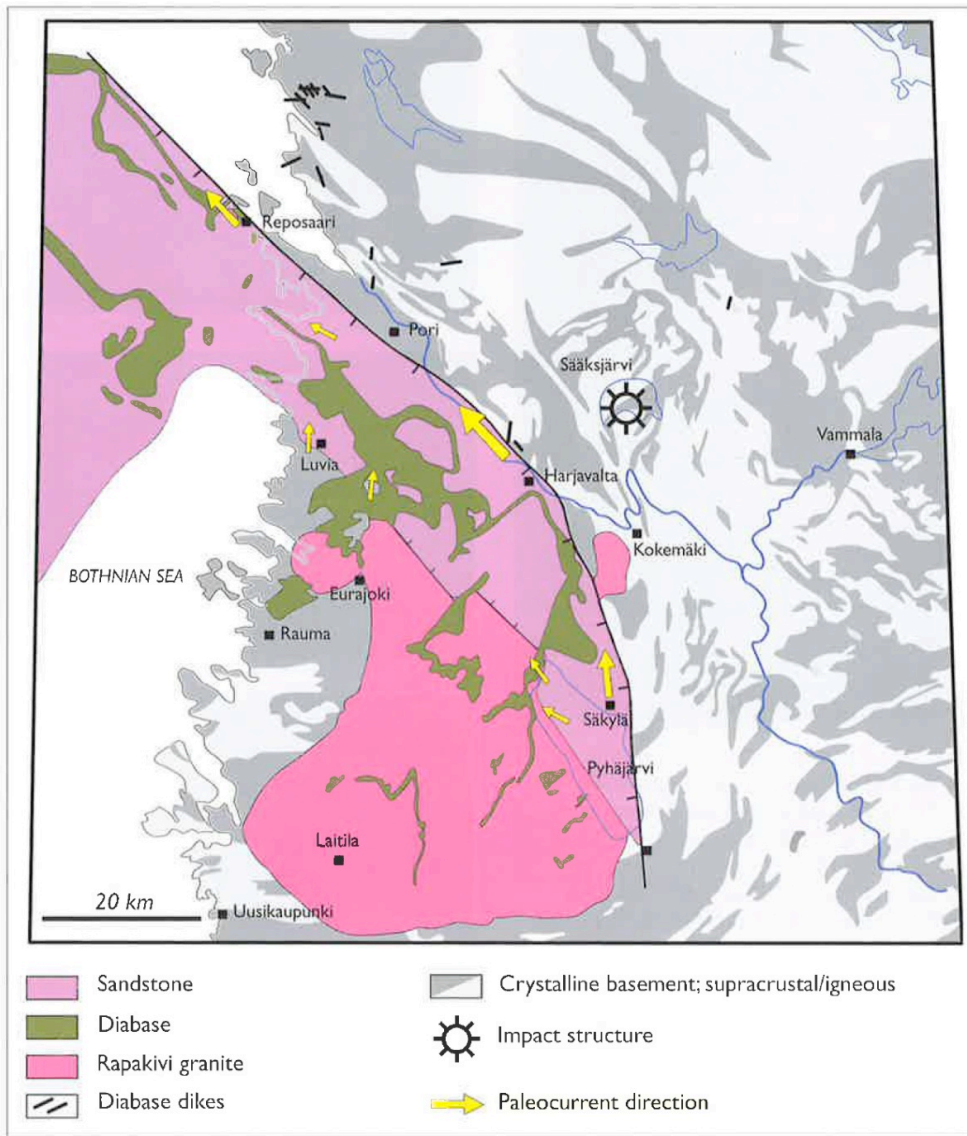


Fig. 13.4. Map of the Satakunta sandstone area in southwestern Finland. The paleocurrent directions are according to Kohonen et al. (1993). For location, see Figure 13.2.

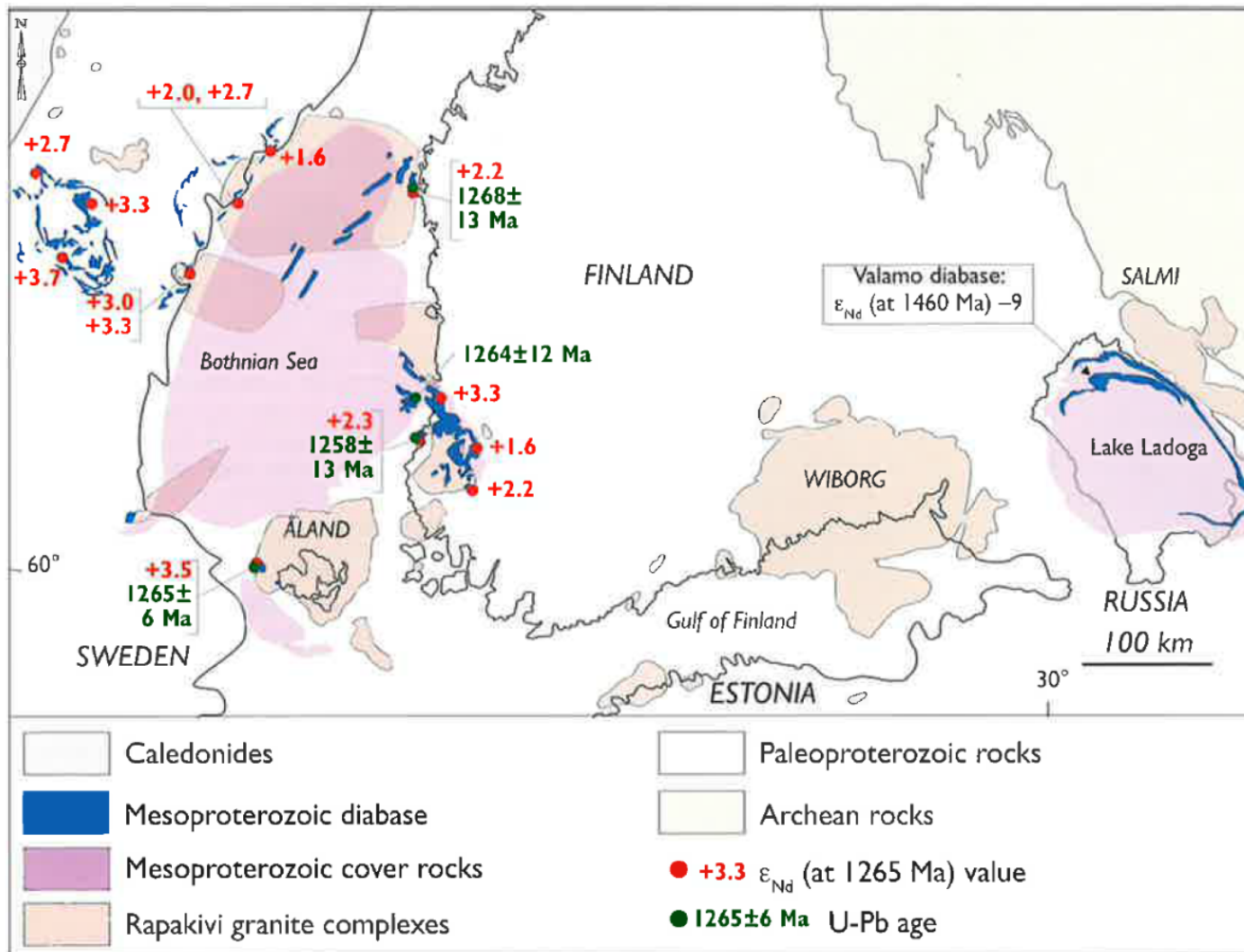


Fig. 13.6. Map showing the distribution of the Mesoproterozoic diabase dikes, cratonic sedimentary cover, and rapakivi granite intrusions in southern Finland and surrounding areas. Initial ϵ_{Nd} values of the diabase dikes (Rämö, 1990; Patchett et al., 1994; this work) are indicated, as are the U-Pb zircon/baddeleyite ages for the Finnish dikes (Suominen, 1991).

Sedimentary cover in Estonia

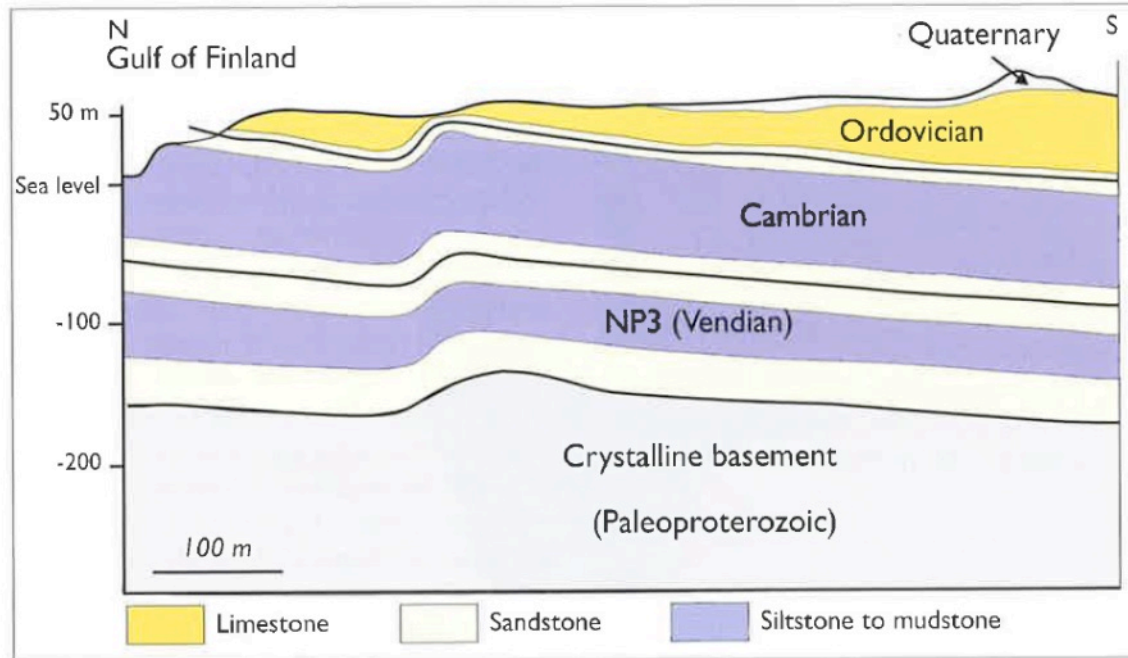
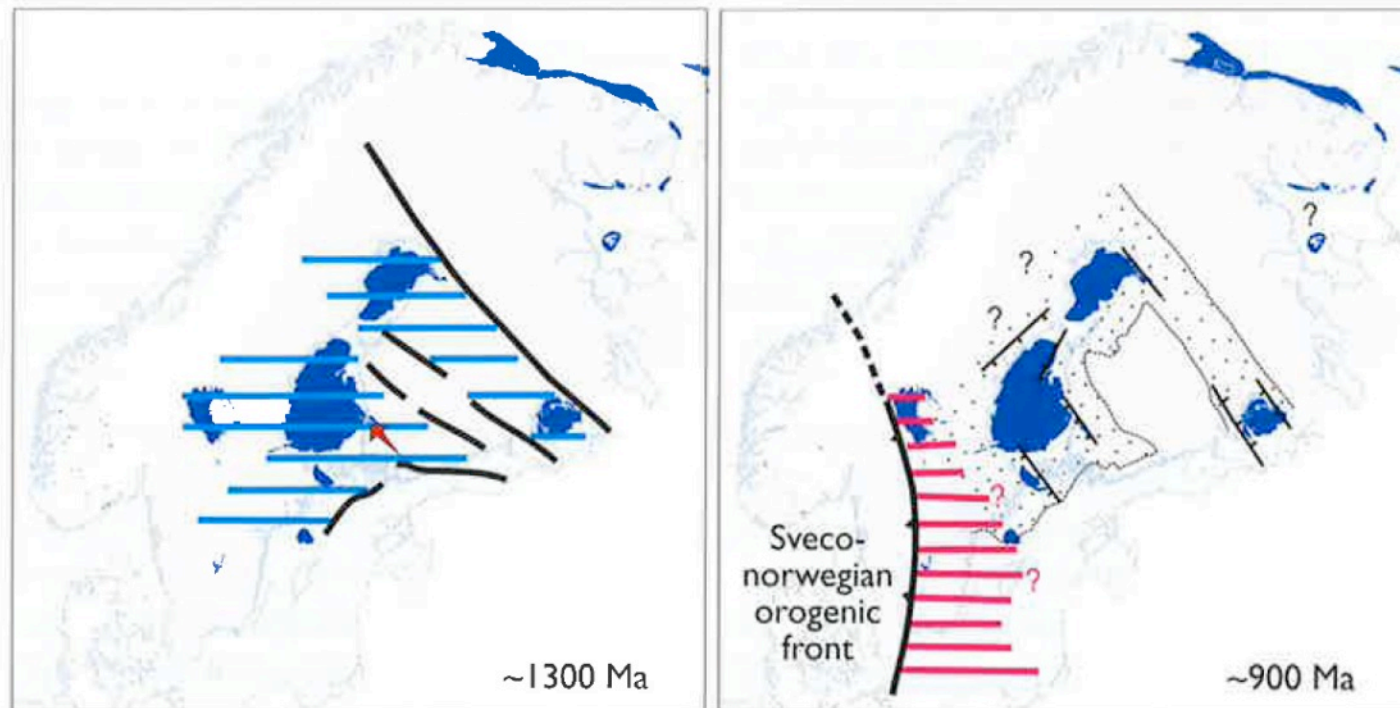
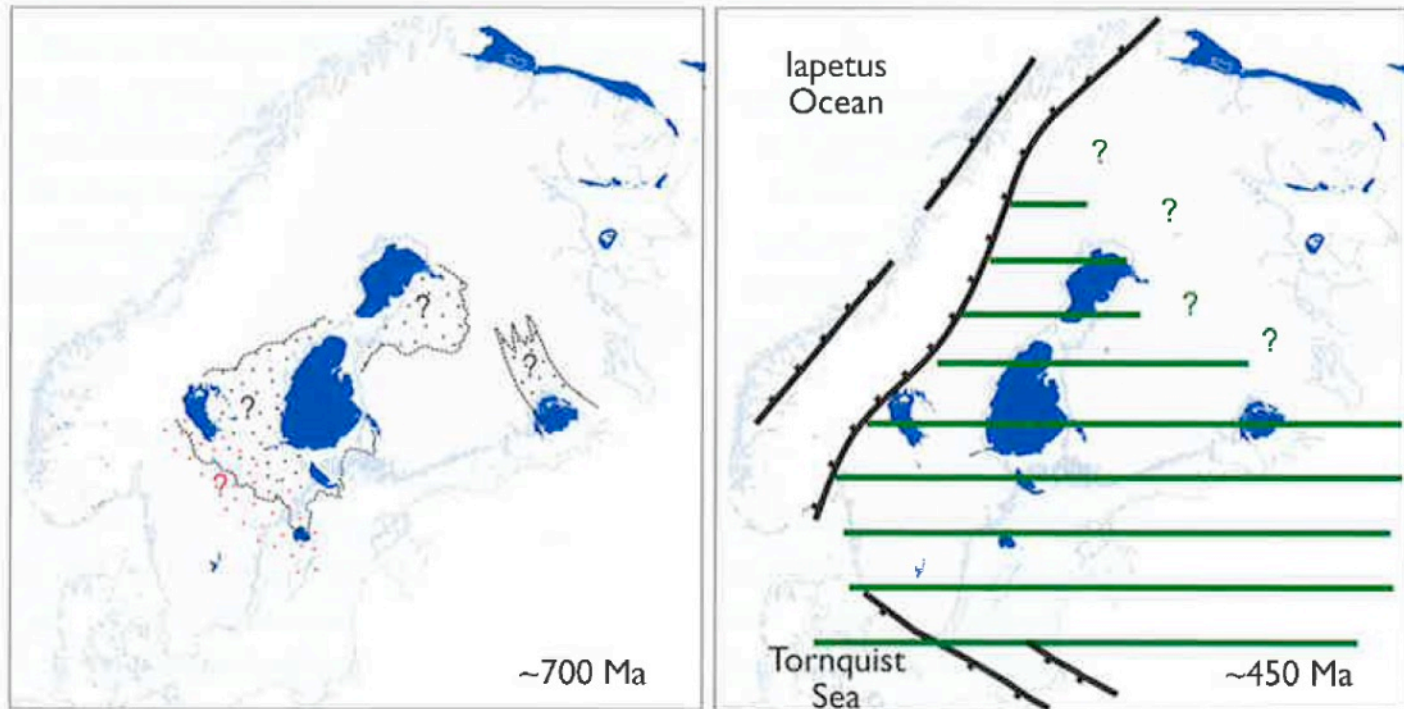


Fig. 13.12. Cross-section showing the uniform thickness of the cover units in northern Estonia to the north of Uljaste (for location see Figure 13.2). Simplified from Puura et al. (1996).

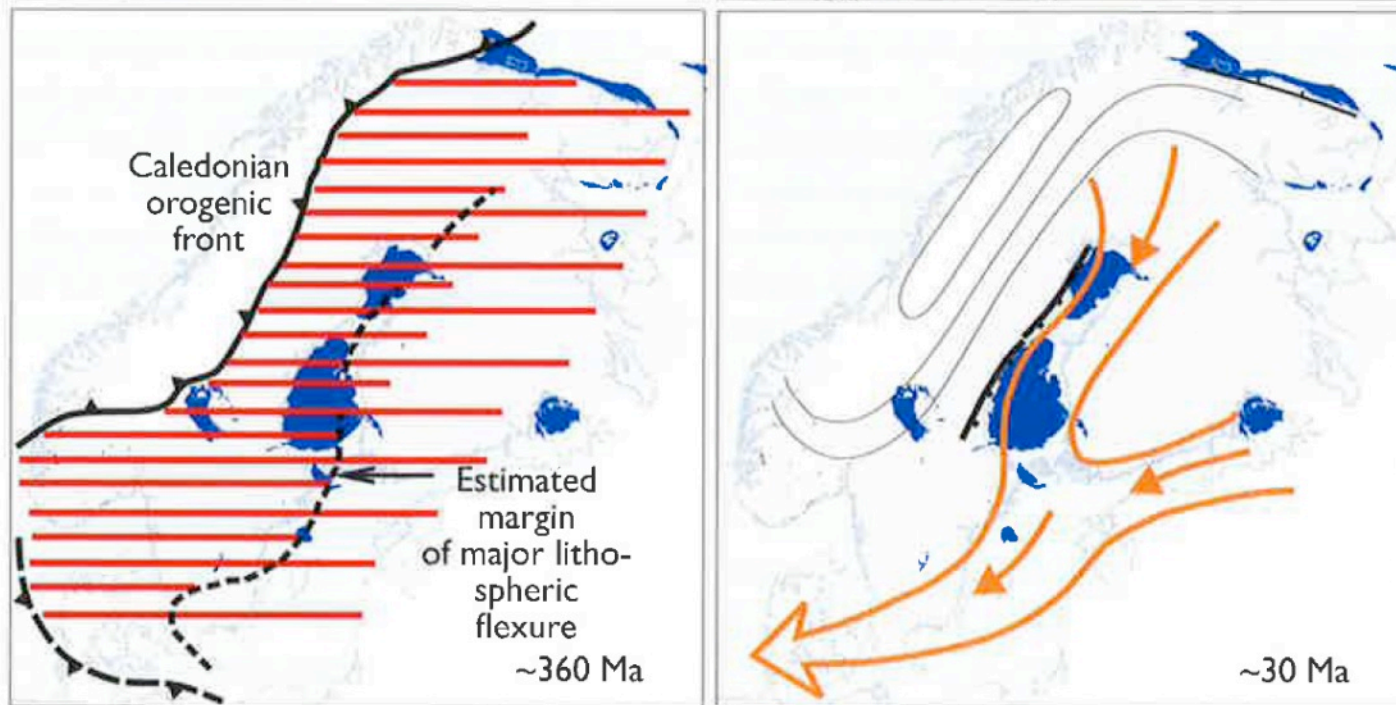
Mesoproterozoic – Paleogene evolution (part 1)

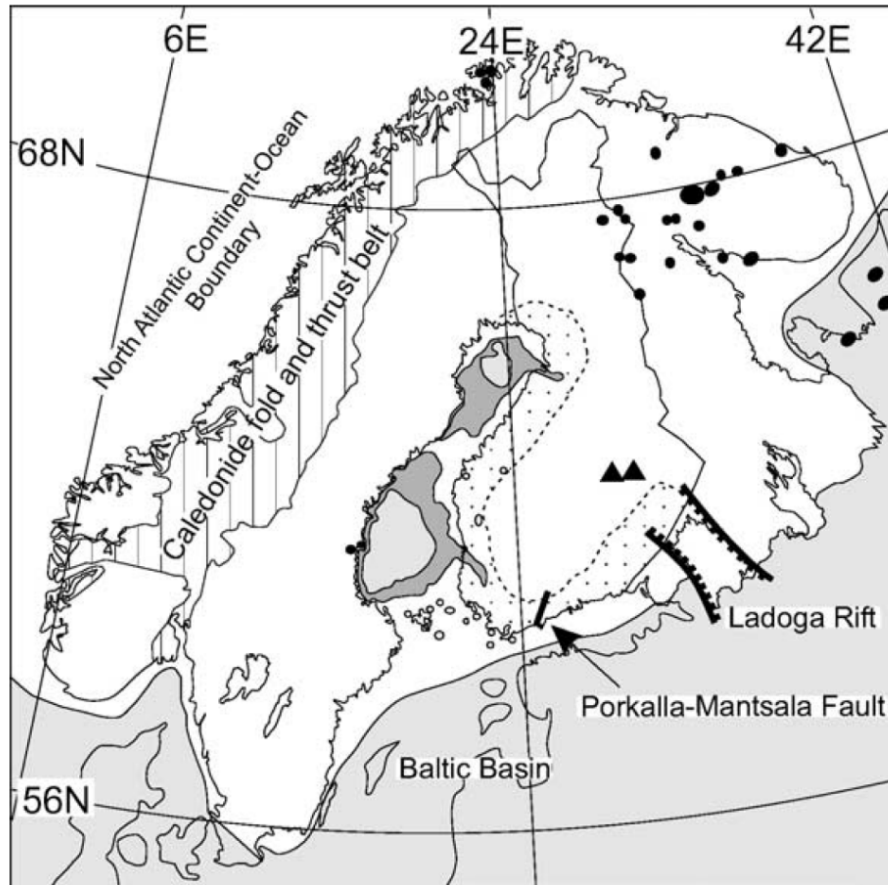


Mesoproterozoic – Paleogene evolution (part 2)



Mesozoic – Paleogene evolution (part 3)



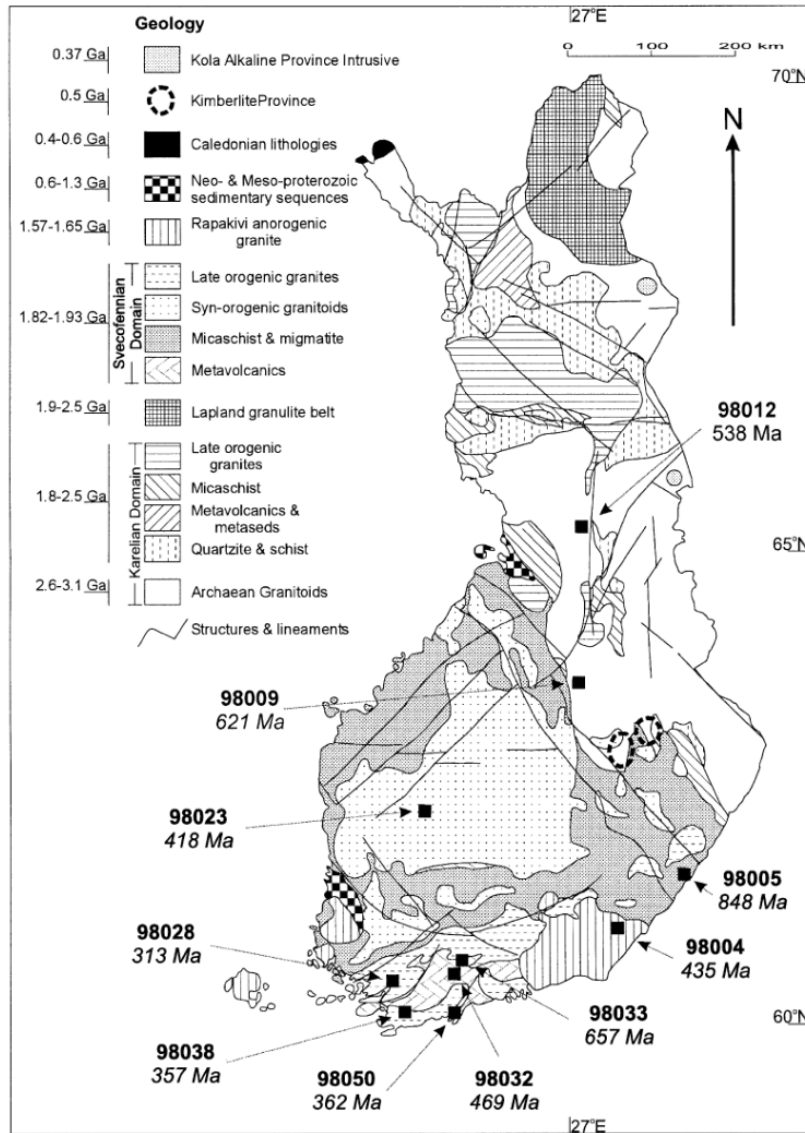


Present day geology

Fig. 1. Present day map of Fennoscandia showing geologic features referred to in the text. Lightly dotted area shows extent of sub-Cambrian peneplain in Finland. Solid grey shows extent of Phanerozoic (light) and Late-Proterozoic (dark) sediments. Black dots show intrusions of the Kola Alkaline Province and black triangles the Kimberlite provinces (taken from Kukkonen and Peltonen, 1999).

Murrell and Andriessen, 2004

Murrell and Andriessen: Sample locations for AFT ages



Murrell and Andriessen: Summary of AFT ages

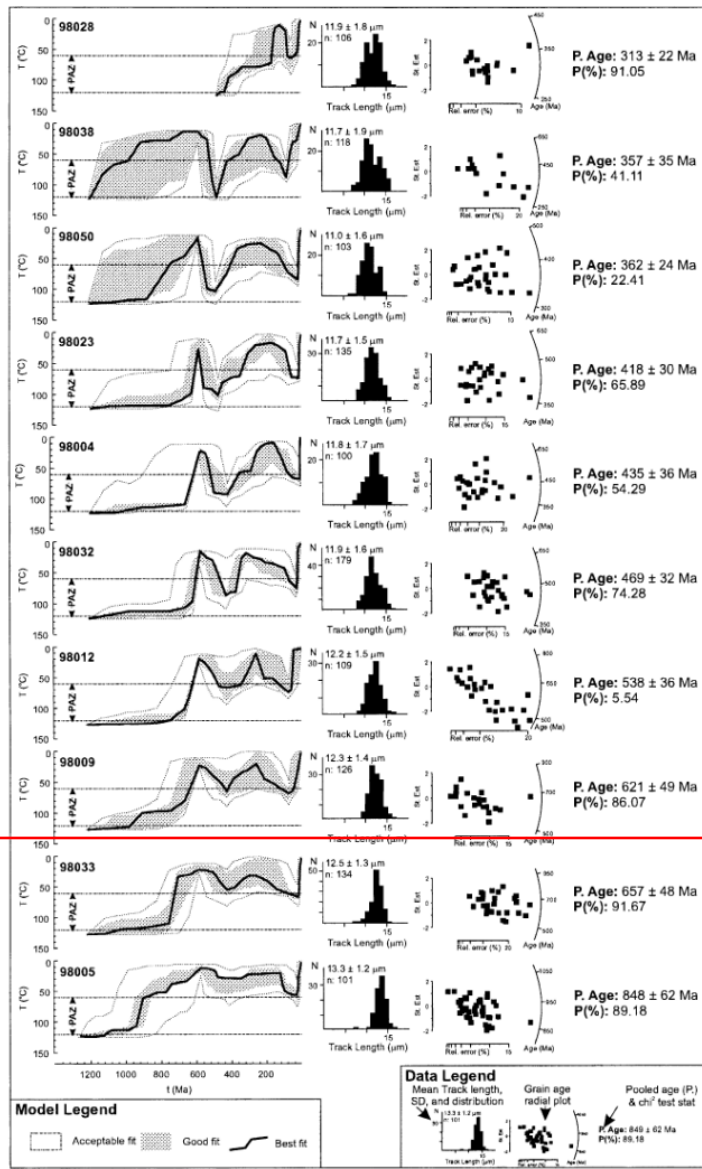


Fig. 3. Showing model results, grain age radial plots and length distributions for each sample.

Enlarged on next page

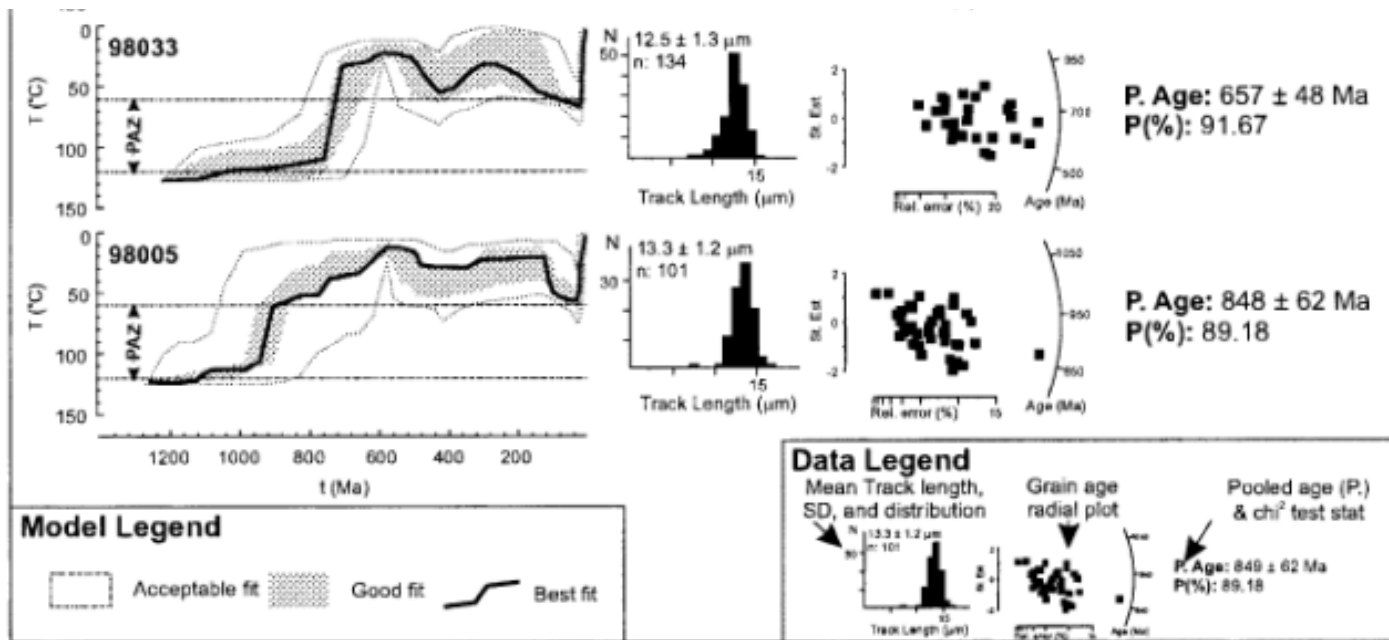
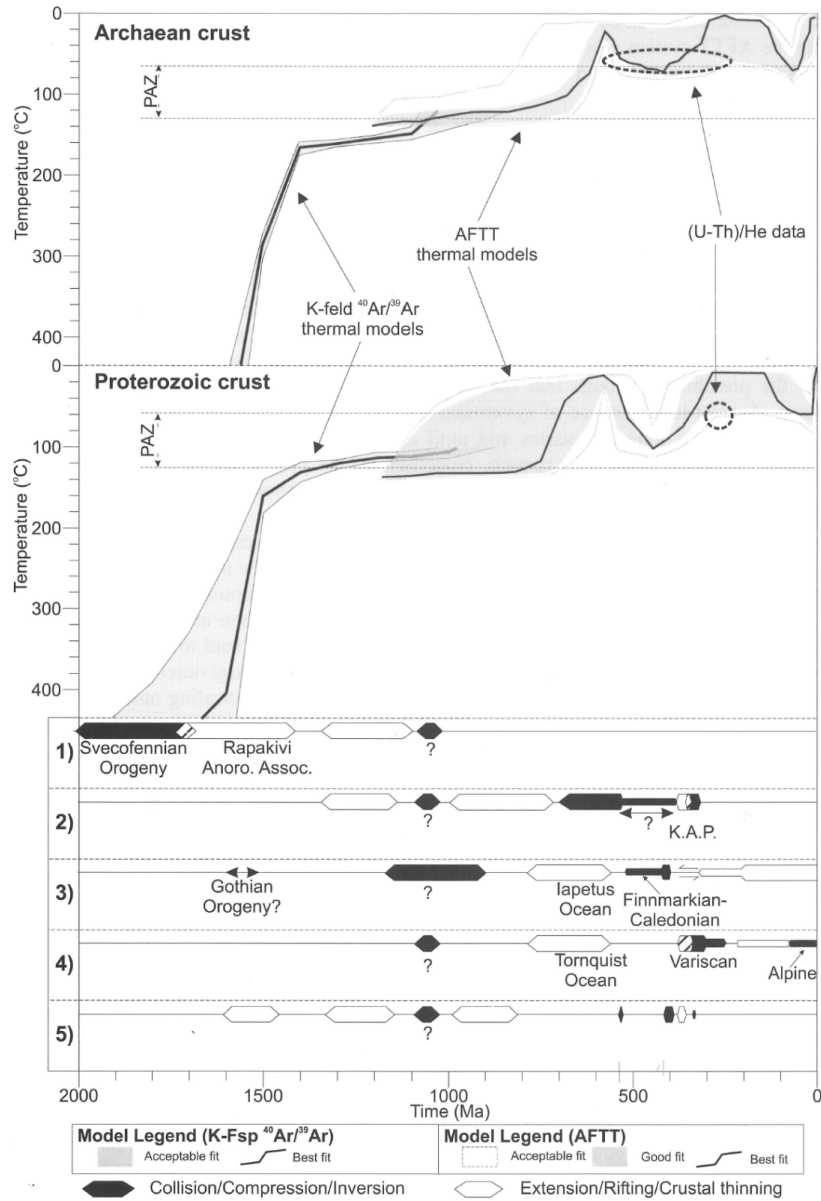


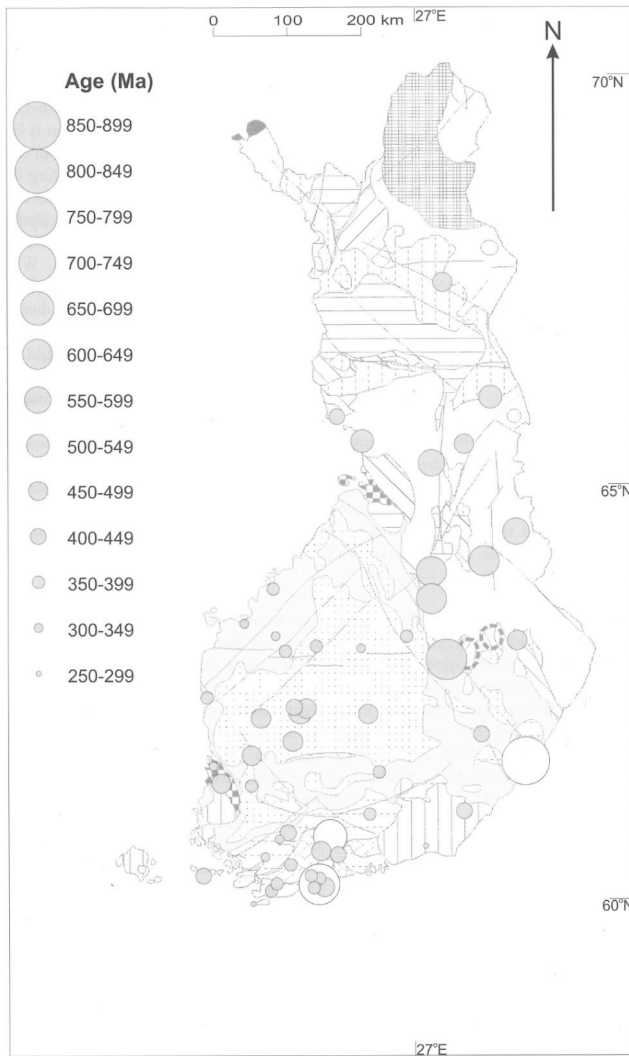
Fig. 3. Showing model results, grain age radial plots and length distributions for each sample.



Murrell 2001:

- Ar-Ar
- AFTT model ages
- (U-Th)/He ages

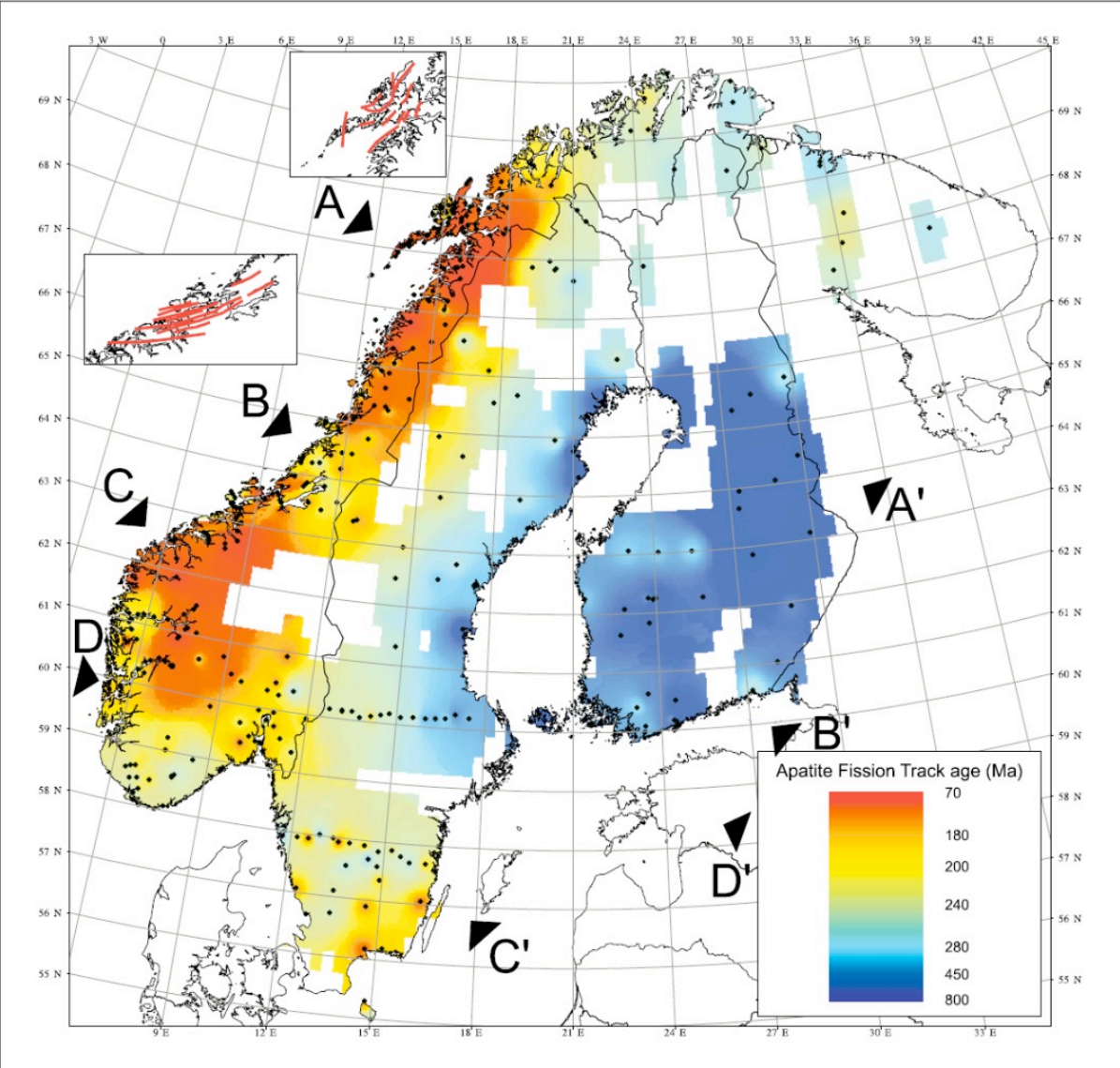
Murrell, 2001



Distribution of AFT ages in Finland

Murrell, 2001

AFT ages in Fennoscandia

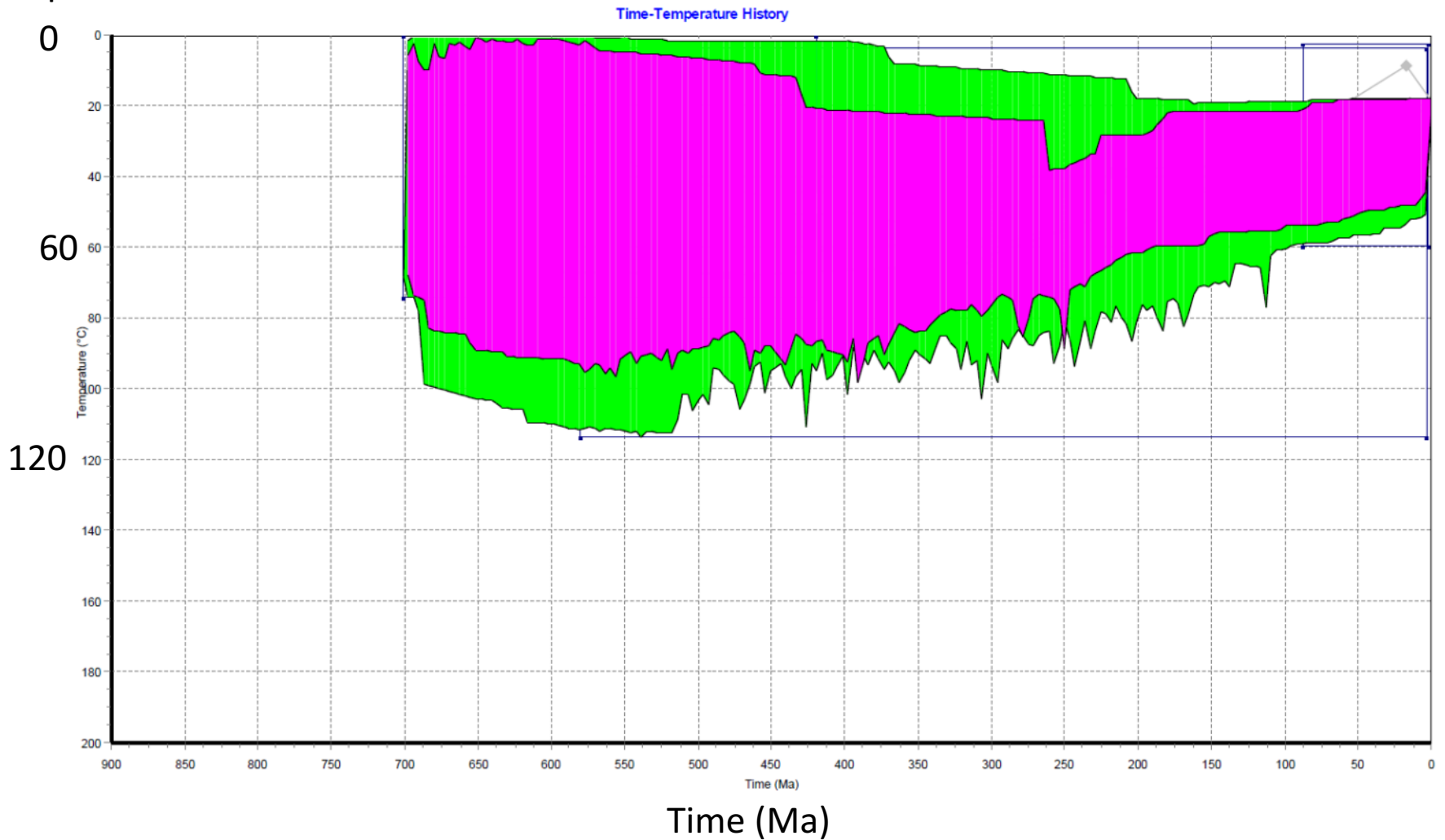


Hendriks et al., 2007

Fig. 3: Pattern of Apatite Fission Track ages in Fennoscandia. Out of a total of 677 available ages, 375 are selected based on elevation, apatite chemistry and analytical approach and data quality (see text for explanation). Areas where no published data exist or where data are excluded as a result of the filtering criteria are blanked. Insets: barrier polylines used as breaklines for contouring. Transects refer to Figure 5. Spatial reference: WGS84, Gauss-Krueger, central meridian 21°E, Latitude of Origin 63°N, false easting 1500 km.

Time-temperature history model Outokumpu 157 m AFTT model (Pecube)

Temperature

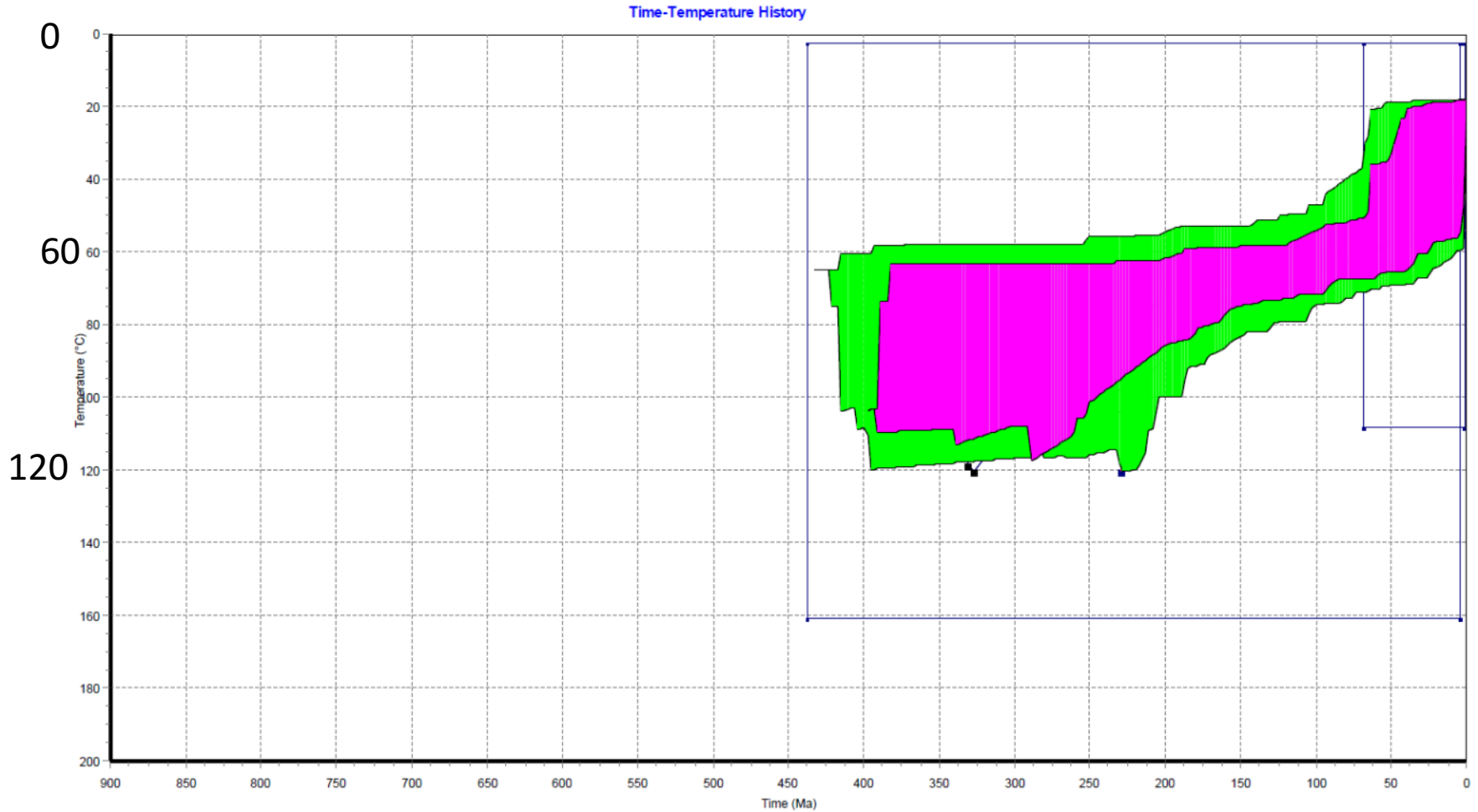


Andriessen and Kukkonen (unpublished)

Ilmo Kukkonen 23.10.2017

Time-temperature history model Outokumpu 1818 m AFTT model (Pecube)

Temperature



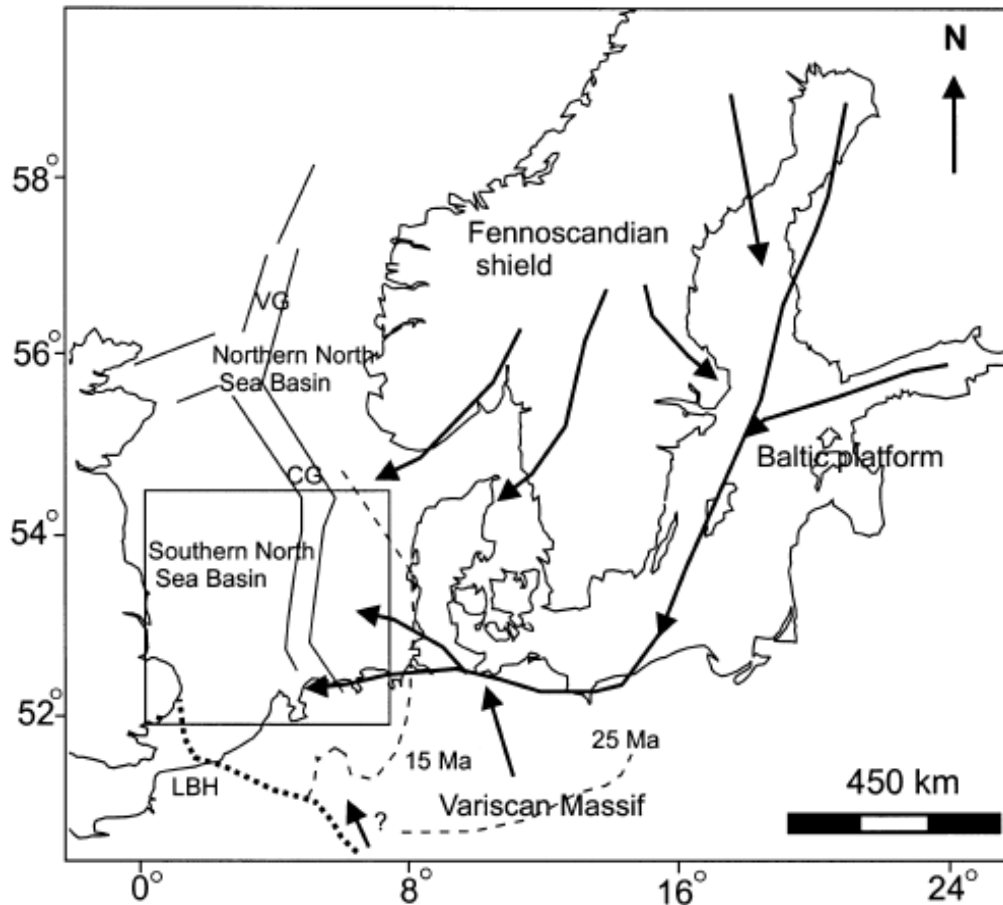
120

Time (Ma)

Andriessen and Kukkonen (unpublished)

Ilmo Kukkonen 23.10.2017

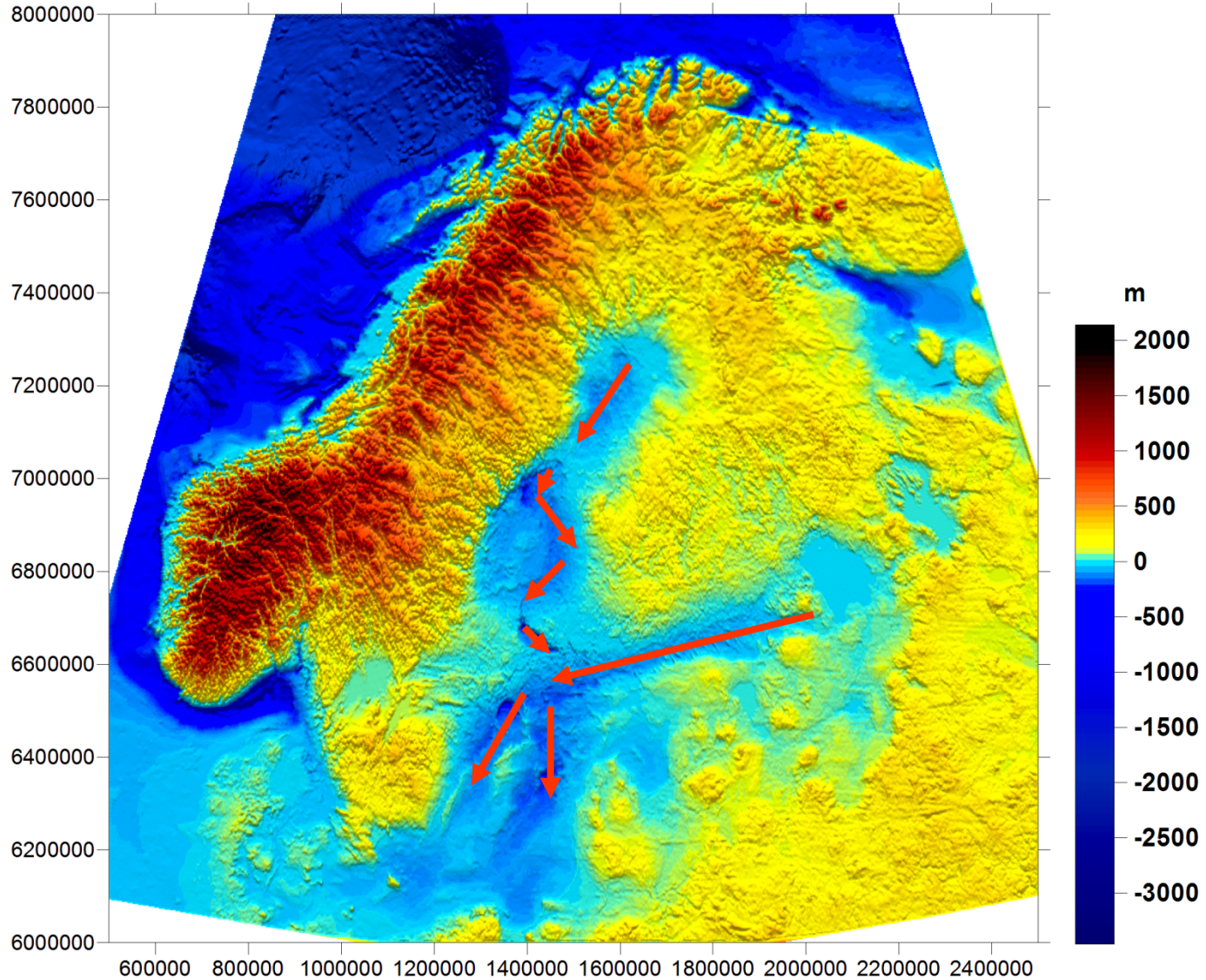
North Sea and Fennoscandia: The *Eridanos* fluvio-deltaic system



- Erosion and transport from Fennoscandia
- Deposition in the North Sea Basin < 10 Ma

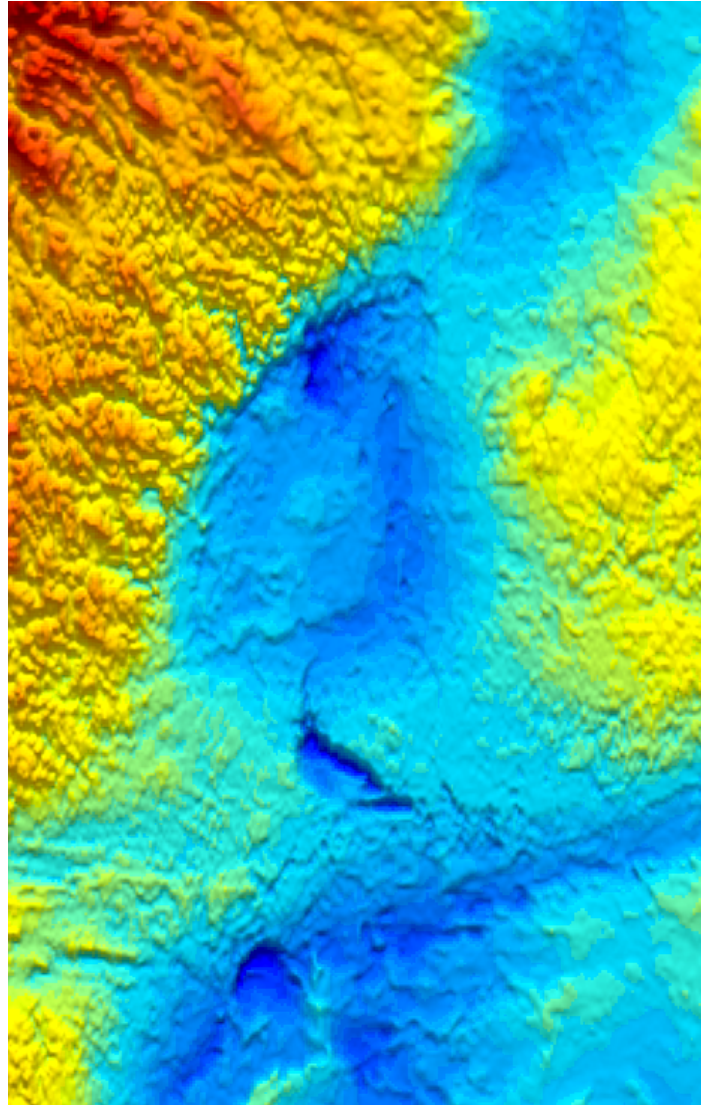
Overeem et al. 2001

Present topography and bathymetry

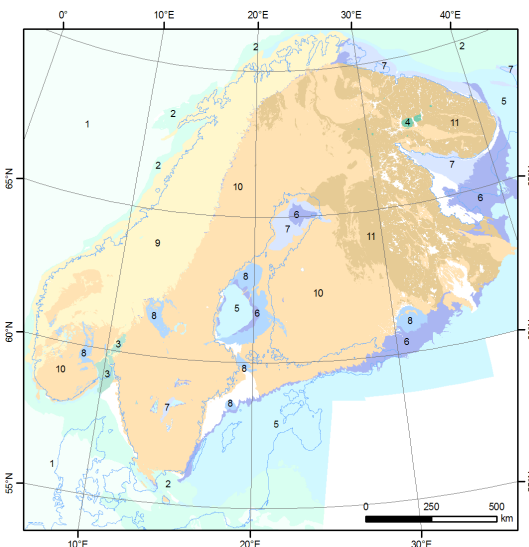
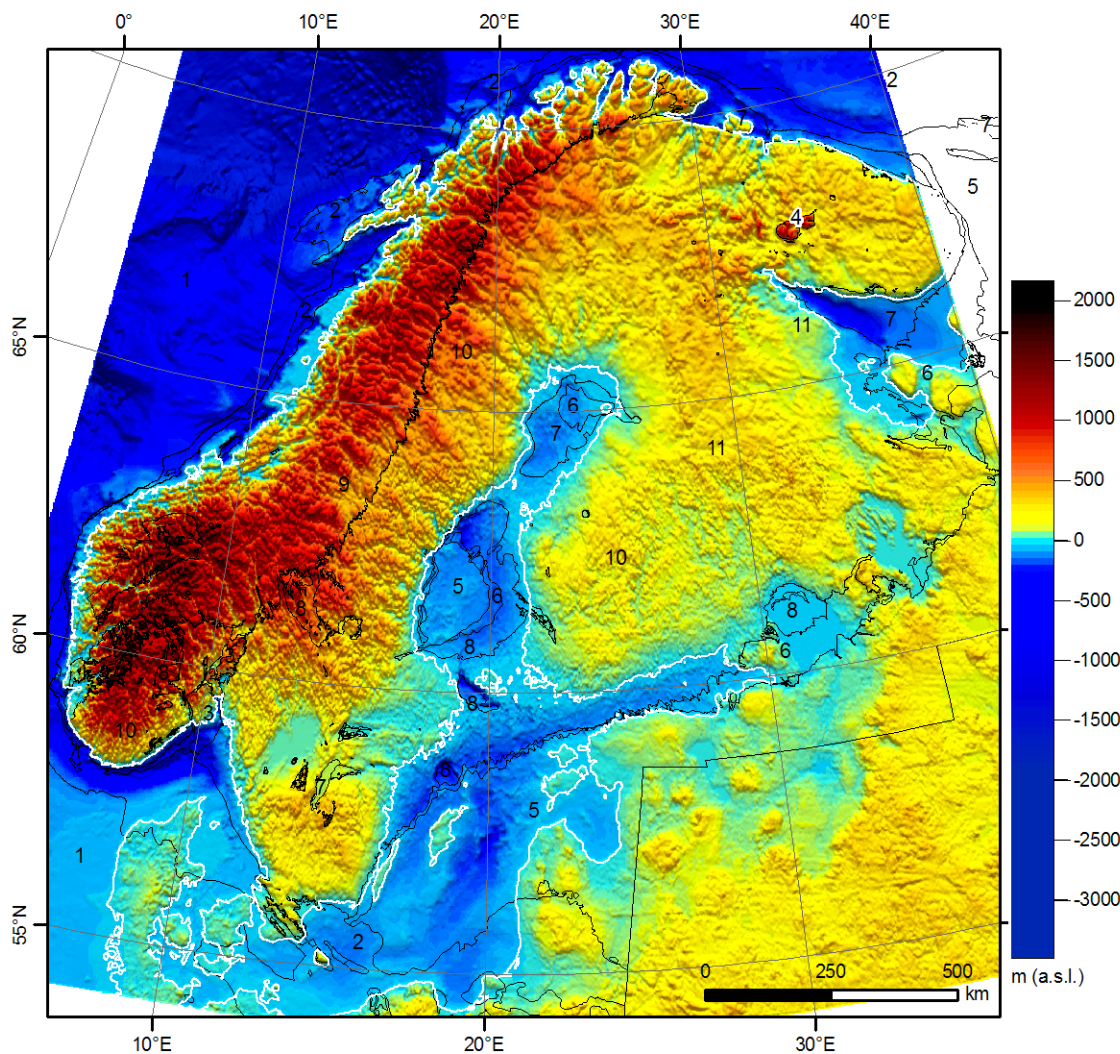


Topographic and bathymetric data from IUGG Data Centre, Boulder (2 arc minute resolution)

Present topography and bathymetry: Detail image



Present topography, bathymetry and major geological units



- | | |
|--|--|
| 1 Cenozoic sedimentary rocks | 7 Upper Riphean and possibly older sedimentary rocks |
| 2 Mesozoic sedimentary rocks | 8 Mesoproterozoic sedimentary rocks (1.50 - 1.30) |
| 3 Permo-Carboniferous sedimentary rocks | 9 Caledonian orogenic belt |
| 4 Devonian igneous rocks | 10 Meso- and Paleoproterozoic crystalline rocks |
| 5 Middle Cambrian to Permian sedimentary rocks | 11 Archaean complex (>2.5 Ga) |
| 6 Vendian to Lower Cambrian sedimentary rocks | no data |

- 5 = Middle Cambrian to Permian
- 6 = Vendian to Lower Cambrian
- 7 = Upper Riphean
- 8 = Mesoproterozoic

Riphean: 1400 – 800 Ma; Mesoproterozoic: 1600 – 1000 Ma

Reminder: Geological time scale

- ← • Age in million of years (Ma)

Eon	Era	Period, subera	Epoch, subperiod	Age (Ma)	
Phanerozoic	Cenozoic	Quaternary Q	Holocene	0.01	
			Pleistocene	1.8	
		Tertiary TT	Pliocene	5.3	
			Miocene	23.8	
			Oligocene	33.7	
			Eocene	54.8	
			Palaeocene	65.0	
	Mesozoic	Cretaceous K	Late	99.0	
			Early	144	
		Jurassic J	Late	159	
			Middle	180	
			Early	206	
		Triassic Tr	Late	227	
			Middle	242	
			Early	248	
		Palaeozoic	Permian P	Late	256
	Early			290	
	Carboniferous C		Pennsylvanian	323	
			Mississippian	354	
	Devonian D		Late	370	
			Middle	391	
			Early	417	
	Silurian S		Late	423	
			Early	443	
	Ordovician O		Late	458	
			Middle	470	
			Early	490	
			Cambrian ε	Merioneth	543
St David's	~1000				
Caerfai	1800				
Proterozoic	Late	Hadrynian		2500	
	Middle	Helikian			
	Early	Aphebian (Canada)			
Archaean	Late	Kenoran	Transvaal	Shamvaian	
	Middle		Witwatersrand	Bulawayan	
	Early		Pongola	Belingwean	
			Pilbara (Australia)	Barberton (S. Africa)	Sebakwian (Zimbabwe)
		Zircons in Jack Hills (Australia)			
	Origin of Earth				~4560

Aikajaksojen suomenkieliset nimitykset

Eon: aioni, puolesta miljardista kahteen miljardia vuotta

Era: maailmankausi, yleensä satoja miljoonia vuosia

Period: kausi, yleensä alle sata miljoonaa vuotta

Epoch: epookki, yleensä kymmeniä miljoonia vuosia

The Baltic Sea and subareas: areas, volumes and depths

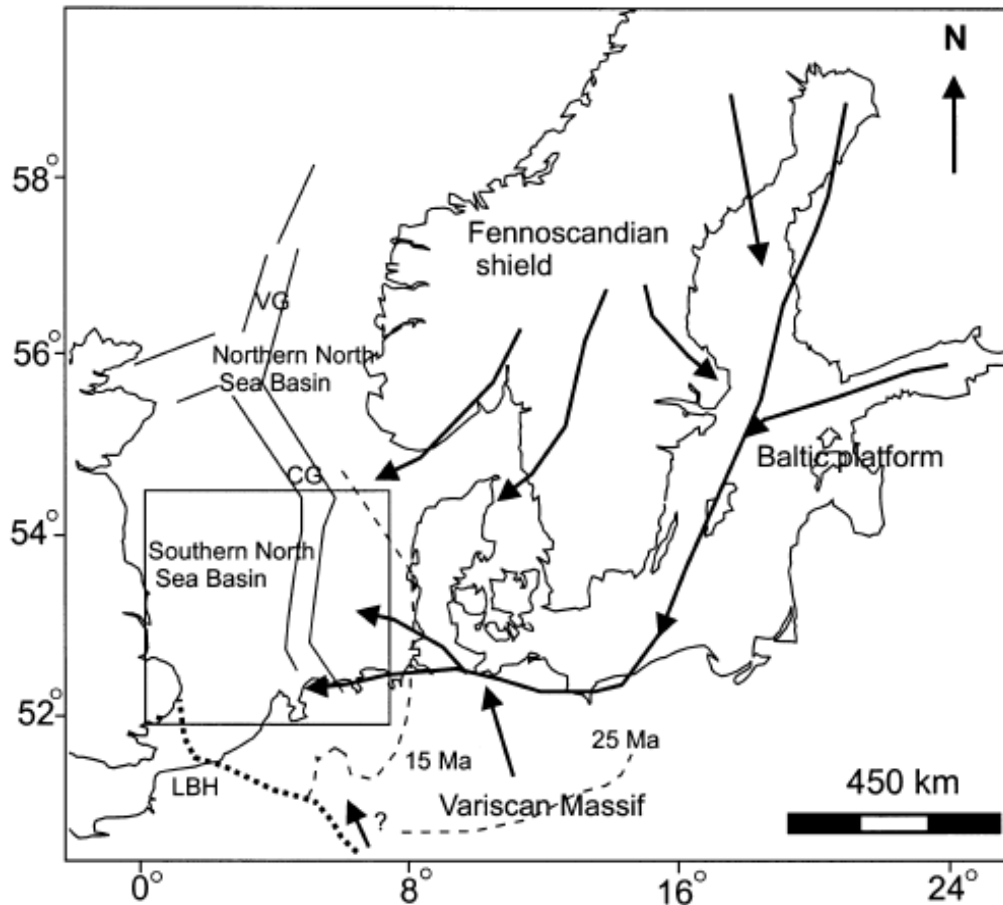
Basin or Deep	Area (km ²)	Volume (km ³)	Max (m)	Mean (m)	Sill depth (m)
Baltic Proper	209,200	13,600	459	67	17
Arkona Basin			55		17
Bornholm Basin			105		45
Gotland Sea			245		60
Gdansk Basin			116		88
Gotland Deep			249		140
Central Basin			219		115
Landsort Deep			459		138
Western Gotland Deep			205		100
Gulf of Riga	18,100	410	51	28	20
Gulf of Finland	29,600	1130	123	38	a
Åland Sea	5200	410	301	77	b
Archipelago Sea	8300	200	104	23	a
Gulf of Bothnia	103,600	5830	294		70
Bothnian Sea	66,000	4340	294	68	70
Bothnian Bay	36,800	1490	147	43	25
Baltic Sea, total	374,000	21,580	459	60	17

a No clear sill.

b Several deep but narrow channels up to 150 m.

Ignatius et al. (1981)

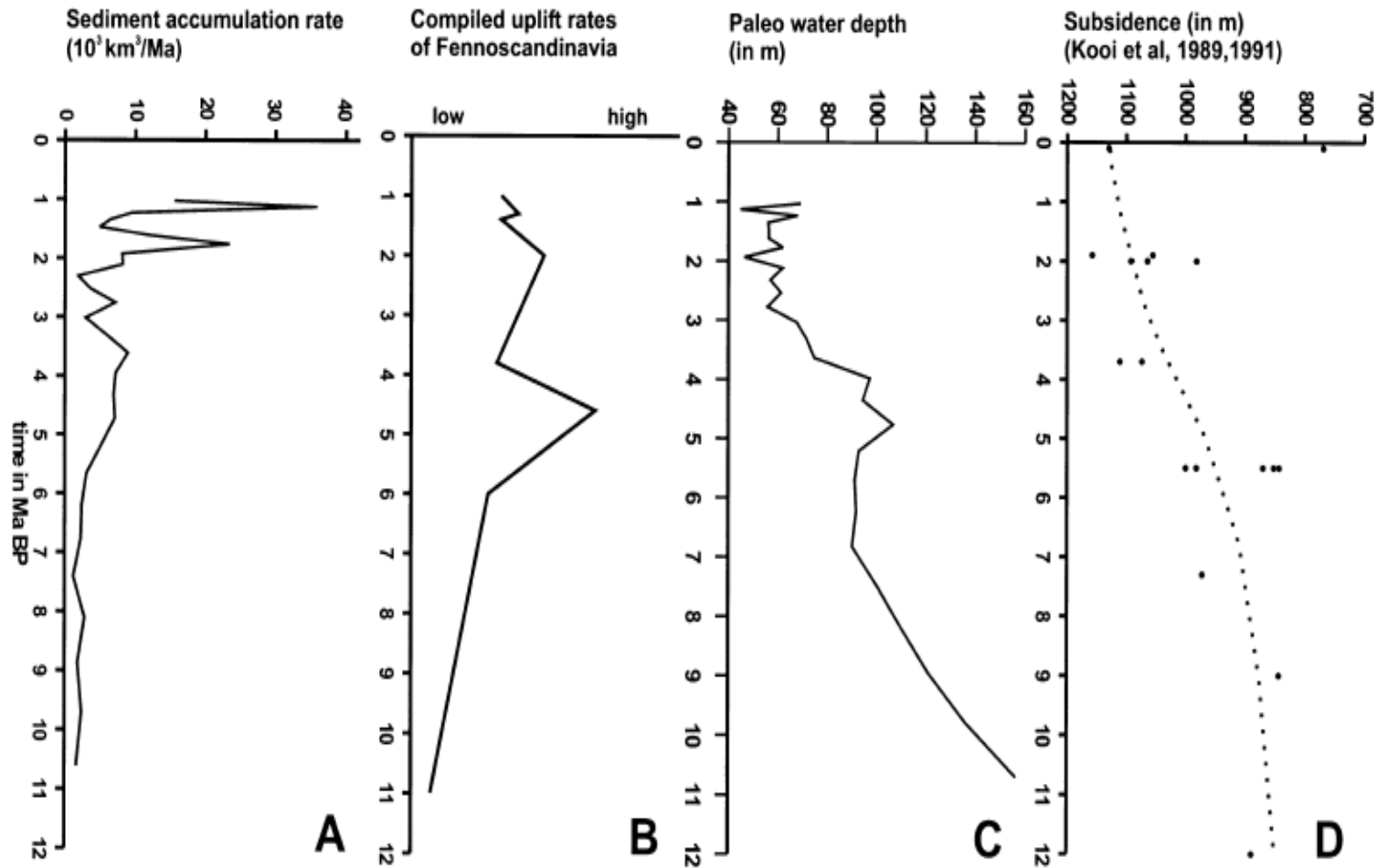
North Sea and Fennoscandia: The *Eridanos* fluvio-deltaic system



- Erosion and transport from Fennoscandia
- Deposition in the North Sea Basin < 10 Ma

Overeem et al. 2001

Pliocene-Pleistocene sedimentation on the Eridanos delta in the North Sea and Fennoscandian uplift



Overeem et al. 2001

Back-of-the-envelope calculation on erosion depths in the last 5 Ma

- Average accumulation rate of sediments in the North Sea $10 \times 10^3 \text{ km}^3$
- Area of the Eridanos river system 1000 km x 200 km
- → about 250 m of rock has been removed

- Average depth of the Baltic Sea and basins is 60 m
- Deep basins 150 – 460 m

- Thus, relatively recent uplift of Fennoscandia and erosion in the Eridanos system would explain the sedimentation rates and young-looking erosional features in the Baltic Sea

It would seem to me that there's a lot of undiscovered issues in low-T thermochronology in Fennoscandia.

Thank you for your attention!